ELSEVIER

Arthropod Structure & Development 34 (2005) 63–87

ARTHROPOD STRUCTURE & DEVELOPMENT

www.elsevier.com/locate/asd

The morphology and vasculature of the respiratory organs of terrestrial hermit crabs (*Coenobita* and *Birgus*): gills, branchiostegal lungs and abdominal lungs

C.A. Farrelly[a], P. Greenaway[b,*]

[a]*32 Tramway Pde. Beaumaris, Vic. 3193, Australia*

[b]*School of Biological, Earth and Environmental Sciences, University of New South Wales, Sydney, N.S.W. 2052, Australia*

Received 23 August 2004; accepted 5 November 2004

Abstract

The morphology and vasculature of the respiratory organs of the terrestrial coenobitids were studied using light microscopy, TEM, SEM and corrosion casting. The gills of *Coenobita* and *Birgus* are modified for air-breathing but are reduced in number and size and have a comparatively small surface area. The branchiostegal lungs of *Coenobita* (which live in gastropod shells) are very small but are well vascularized and have a thin blood/gas barrier. *Coenobita* has developed a third respiratory organ, the abdominal lung, that is formed from highly vascularized patches of very thin and intensely-folded dorsal integument. Oxygenated blood from this respiratory surface is returned to the pericardial sinus via the gills (in parallel to the branchiostegal circulation). *Birgus*, which does not inhabit a gastropod shell, has developed a highly complex branchiostegal lung that is expanded laterally and evaginated to increase surface area. The blood/gas diffusion distance is short and oxygenated blood is returned directly to the pericardium via pulmonary veins. We conclude that the presence of a protective mollusc shell in the terrestrial hermit crabs has favoured the evolution of an abdominal lung and in its absence a branchiostegal lung has been developed.

Keywords: *Coenobita*; Anomura; Land crab; Lungs; Gill; Circulation

1. Introduction

The terrestrial hermit crabs (Family Coenobitidae) include 15 species of *Coenobita* and a single species of another genus, *Birgus latro*. The family is of marine origin and whilst its members have effectively colonised supralittoral and terrestrial habitats, they continue to carry and live in mollusc shells. However, *B. latro*, which carries a shell in its early stages, discards it after several moults, which allows it to grow to a much larger size (Harms, 1938). These shell-less individuals have enlarged and heavily calcified abdominal terga to protect the abdomen and the abdominal integument becomes thick and rubbery.

Whilst extensive work has been conducted on the respiratory physiology of the highly terrestrial *Birgus latro*, relatively little information is available for *Coenobita* (see review by Greenaway, 2003). Furthermore, little seems to be known about the morphology of the respiratory structures involved or their relative contributions. In comparison to terrestrial brachyurans, the terrestrial anomurans (except *Birgus latro*) have fairly reduced branchiostegites, with development constrained by the need to accommodate the body within a gastropod shell. They also retain a large number of gills (14 pairs), and although these are reduced in size (Harms, 1932) it has been assumed that the gills remain the major respiratory organs. The occurrence of a third respiratory site was briefly reported by Bouvier (1890a) for *Coenobita clypeatus* (formerly *C. diogenes*) and comprises a vascular network in the thin dorsal integument of the abdomen. The existence of similar abdominal complexes has also been reported in *C. perlatus* and *C. rugosus* (Borradaile, 1903). Although these systems were discussed by Harms (1932), they have received no

* Corresponding author. Tel.: +61 2 9313 7730; fax: +61 2 9385 1558.
E-mail address: p.greenaway@unsw.edu.au (P. Greenaway).

1467-8039/$ - see front matter © 2004 Elsevier Ltd. All rights reserved.
doi:10.1016/j.asd.2004.11.002

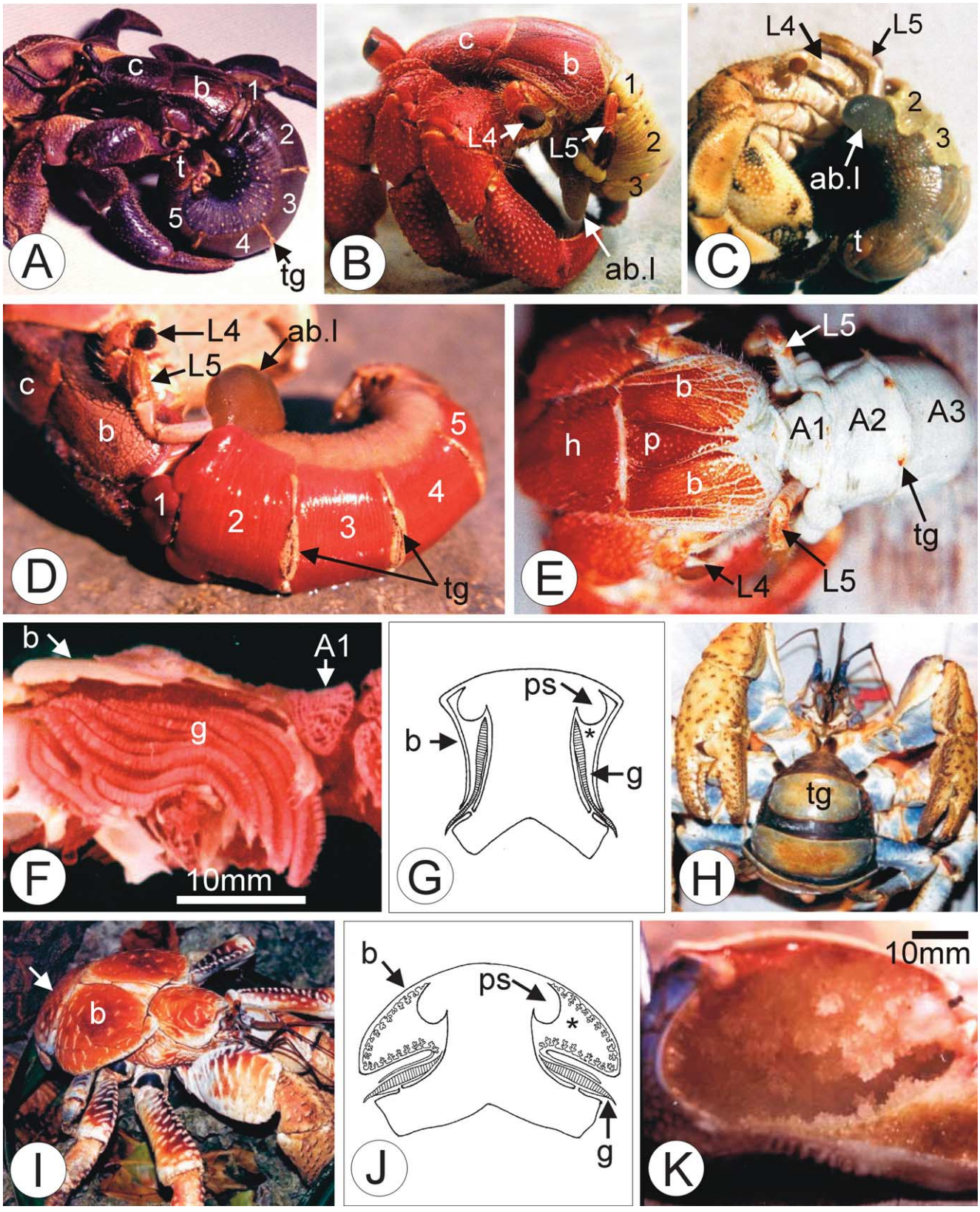

Fig. 1. (A) *Coenobita brevimanus*; (B) *Coenobita perlatus*; (C) *Coenobita rugosus*; (with gastropod shell removed). Note narrowly compressed cephalothorax (c). The 4th limb (L4) is held against the sides of the branchiostegites (b), while the 5th limb (L5) is normally inserted into the branchial chamber. The abdomen is covered with a thin, membranous cuticle and the abdominal tergites (tg) are reduced to narrow bars between the segments. The last segment and telson (t) are reduced and calcified. Distinctive vascular patches on the abdomen extend dorsally and mid-laterally where the surface forms tiny grooves that run laterally

subsequent attention and the potential contribution of the abdominal gas exchange site to the physiology of gas exchange in terrestrial hermit crabs has been ignored.

In this study, we describe in detail, using modern techniques, the anatomy of the three different respiratory structures present in the two genera of terrestrial coenobitids. The major objective was to assess the anatomical suitability of each respiratory organ for gas exchange and thereby establish their probable respiratory importance. A second objective was to establish the detailed anatomy of the respiratory circulations in *Birgus* and *Coenobita* and a third was to use the anatomical information gained to determine how the use of gastropod shells has affected gas exchange and respiratory circulation in coenobitids.

2. Materials and methods

2.1. Species investigated

Small specimens of the highly terrestrial *Birgus latro* (Linnaeus, 1767), *Coenobita brevimanus* (Dana, 1852) *C. perlatus* (Milne-Edwards, 1837) and *C. rugosus* (Milne-Edwards, 1837) were collected on Christmas Island and taken to the Christmas Island field station and processed for scanning electron microscopy (SEM), transmission electron microscopy (TEM) or corrosion casting. *Birgus* is found across the island, whilst *Coenobita* appears to be restricted to the island's lower terraces, closer to the sea. *C. rugosus* and *C. perlatus* occupy the lowest part of the sea terrace including the beach, whilst *C. brevimanus* ventures some 500 m inland and is most often found in the rainforest.

2.2. Corrosion casts

Corrosion casts of the vasculature were made by injecting six animals of each species with Batson's #17 Anatomical Corrosion Compound (Polysciences Inc., Warrington, PA). Soft tissues were digested away with sodium hypochlorite. The casts were photographed with a macro lens and portions of the casts were metal coated and examined with a JEOL JSM 6340F field emission scanning electron microscope.

2.3. Microscopy

For light microscopy and TEM, branchiostegal and abdominal tissues were cut into very small pieces and fixed for 2 h in 2.5% glutaraldehyde buffered with 0.1 mol l^{-1} Na cacodylate and NaCl (pH 7.2; osmotic pressure ~850 mosmol) and then post-fixed in 2% OsO_4 in the same buffer. The tissue was then embedded in Spurr's resin and sectioned for light microscopy and TEM on a Leica Ultracut UCT ultramicrotome using glass or diamond knives. Semi-thin sections were stained with 0.5% toluidine blue in 1% borax and photographed using a Zeiss Axioskop2 microscope. Ultrathin sections were double stained with lead citrate and uranyl acetate and examined in a Hitachi H600 TEM. Freshly dissected gills were also prepared for SEM by fixing in 2.5% glutaraldehyde buffered with 1 mol l^{-1} Na cacodylate, and then critical-point dried. The gills were then mounted on stubs, metal coated and examined in a Hitachi S4500II SEM.

2.4. Surface area of branchiostegal lungs

The surface area of the branchiostegal lungs was estimated from corrosion casts. Paper patterns of the branchiostegites were cut out; their outline was copied onto mm-ruled graph paper and scanned into the computer. These images were then enlarged and the number of square millimetres in each outline was counted and summed.

2.5. Surface area of abdominal lung

The surface area of the abdominal lung was estimated from both light micrographs (number of respiratory grooves/cm, average depth of grooves and distance between grooves) and from casts (transverse length of grooves and length of each respiratory segment). It was assumed that the walls of the grooves formed perfect rectangles, with two equal sides. Thus the surface area of each respiratory groove

across the abdomen and are indicated by numerals corresponding to the abdominal segment. ab.l, abdominal lobes. (D) *Coenobita brevimanus* injected with corrosion casting plastic showing distinctive dorsal vascular patches (numbered) on abdomen, including the pedicel (segment 1) and the contractile abdominal lobes (ab.l). Note densely packed grooves on the dorsal surface of abdomen. b, branchiostegites; c, cephalothorax; L4, fourth thoracic limb; L5, fifth thoracic limb; tg, reduced tergites. (E) *Coenobita perlatus*, (dorsal view), showing extreme lateral compression of body. Note that the branchiostegites (b) barely exceed the width of the head region (h). Vascularized abdominal segments are numbered, including the pedicel (A1); L4, Fourth thoracic limb; L5, Fifth thoracic limb; p, pericardial region; tg, reduced tergites. (F) *Coenobita brevimanus*, lateral view of cast with tissues partially removed. The branchiostegites (b) have been cut away to reveal the gills (g), which almost fill the branchial chamber, (the tips of the gills almost reach the roof of the branchial chamber). A1, pedicel (first abdominal segment). (G) Schematic diagram of vertical section through *Coenobita*, showing the very limited lateral extension of the branchiostegites (b) forming the branchial chambers, which are essentially filled by the gills (g) and the pericardial sacs (ps). Note the extremely narrow lumen of the branchial chambers (*) (H) *Birgus latro*, ventral view, showing the large abdomen covered with a thick rubbery integument and protected dorsally by large, individual heavily calcified tergites (tg). (I) *Birgus latro*, lateral view, showing the narrow head region and the broad, dorsally expanded branchiostegites (b) that form the lungs. The first heavily calcified abdominal tergite can also be seen (arrow). (J) Schematic diagram of vertical section through *Birgus*, showing the broad lateral extension of the branchiostegites (b), folded to form an expansive, upper lung chamber (*) and a lower, smaller gill chamber. The two chambers are almost completely separated by the branchiostegal fold, (folded inwards to form the lung floor and folded outwards to cover the gills (g)). ps, pericardial sacs. (K) The right branchiostegite of *Birgus latro* removed and viewed from the lumen side. Note the lining of the upper lung chamber has been greatly expanded by highly branched respiratory lobes that cover the surface and project into the lung lumen.

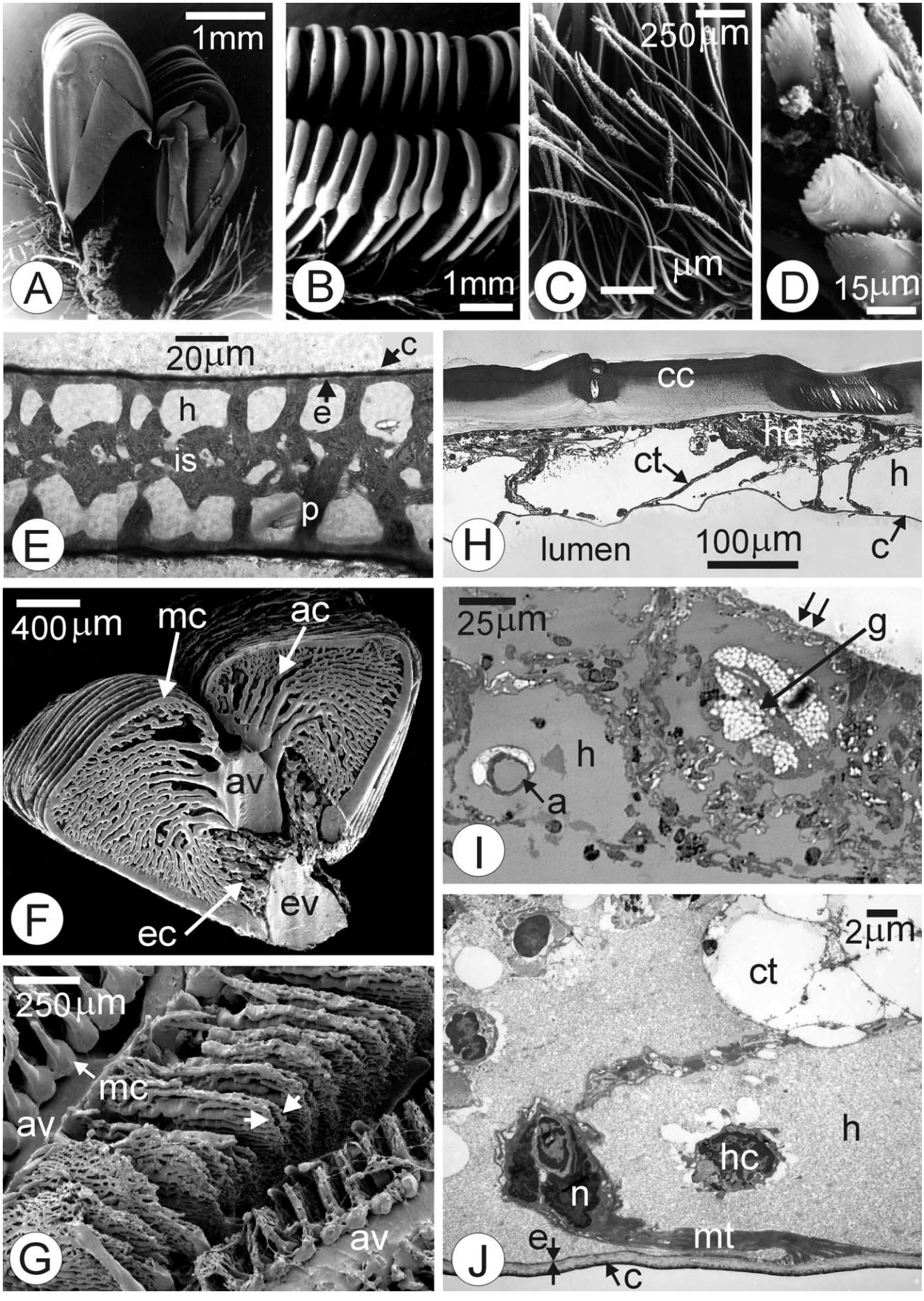
A
1mm
B
1mm
C
250µm
µm
D
15µm
E
20µm
c
h
e
is
p
H
cc
hd
ct
h
lumen
100µm
c
F
400µm
mc
ac
av
ev
ec
I
25µm
g
h
a
G
250µm
mc
av
av
J
2µm
ct
h
hc
n
mt
e
c

is the sum of three rectangles (two lateral walls, plus the surface of the tip), multiplied by the number of grooves/-segment. The surface area of each segment was then summed to give the total surface area of the abdominal lung.

3. Results

3.1. The branchial chamber

The respiratory organs were very similar in structure in all three species of *Coenobita* studied. Therefore, the results for this group are presented and described in general terms, unless otherwise stated.

In *Coenobita*, the maximum width of the body is constrained by the dimensions of the gastropod shell and thus the entire body is narrow and compact (Fig. 1(A)–(D)). The forepart of the cephalothorax is laterally compressed, with a narrow, vaulted roof and flat vertical sides (Fig. 1(A)). Its compression extends also to the first three pairs of legs, so that the whole complex can be withdrawn into the shell. Anteriorly, the branchiostegites are compressed and calcified and house the scaphognathite, but posteriorly they are soft and tend to be depressed. The fourth pair of legs is carried pressed up against the sides of the body, indenting the soft branchiostegites (Fig. 1(C) and (D)). The branchiostegites only project dorsally and posteriorly where they overhang the limbs, gaping posteriorly and making the gills partially visible. The fifth pair of legs is thrust through this opening into the gill chamber (Fig. 1(E)). The free edge of the branchiostegite is curved over the gills and its margin is lined with hairs. The lateral expansion of the upper part of the branchial chamber is constrained by available shell size. Consequently, the lumen of the branchial chamber is almost entirely filled by the gills, which lie against the steeply sloping epimerites (Fig. 1(F) and (G)) and by the large pericardial sacs that extend along the lateral edge of the pericardial sinus (Fig. 1(G)).

In *Birgus*, the carapace and branchiostegites are not restricted by a gastropod shell and the abdomen is protected by heavily calcified dorsal terga (Fig. 1(H)). The head and anterior thorax are encased in a rigid and narrow carapace (Fig. 1(I)) and its lateral (branchiostegal) walls are folded inwards ventrally, forming a narrow channel on each side that houses the scaphognathites. Over the posterior thorax the carapace is extended laterally (Fig. 1(I)). In this region the branchiostegites are folded in on themselves to form two almost separate compartments, an upper, expansive lung chamber and a lower, smaller gill space (Fig. 1(J)). The upper chamber is extended laterally into broad wings with distinct dorsal and ventral surfaces (Fig. 1(J)). The lower branchial space is enclosed dorsally by the fold of the branchiostegite that extends to the coxae of the legs. The floor of the branchial space is formed by the sloping thoracic epimerites and the lumens of the lung and the branchial space are connected by a narrow slit. More posteriorly, the separation of the lungs from the gills gradually decreases allowing space for the fifth pair of thoracic legs to enter the lung chamber. In *Birgus*, the dorsal and ventral lung surfaces are covered with small branching, tree-like evaginations (Fig. 1(K)). As in *Coenobita*, large pericardial sacs extend along either side of the pericardial sinus and occupy the inner, dorsal portion of the lung.

3.2. Gills

3.2.1. External morphology

Coenobitids, including *Birgus* have phyllobranch type gills. The axis of each gill is divided into two from a middle attachment point, with each side bearing a series of paired small, thin-walled lamellae that diminish in size towards each end of the axis to form a spindle shaped gill (Fig. 1(F)). The gill number and formulae of the terrestrial coenobitids are the same as those of the aquatic pagurids (14 pairs) (Borradaile, 1903; Harms, 1932), however, the gills are very much reduced in size, with fewer lamellae (Harms, 1932). The anterior four gill pairs are extremely difficult to identify and consist of only one or two bubble-like lamellae with

Fig. 2. (A–D) Scanning electron micrographs of *Birgus* gills. (A) Cross-sectional view through gill showing the small ovate lamellae and the long hairs that surround their ventro-lateral margins (ventral edge of gill was damaged during preparation). (B) Dorso-lateral view of gill; note expanded marginal canals bearing a row of nodules on each side. (C–D) SEM pictures showing the complex structure of the hairs that line the ventral surface of the gill shaft. Each hair comprises a long slender shaft and a head of toothed scales. (E) *Coenobita perlatus*, light micrograph of epoxy section through the lamella of gill 12. The cuticle (c) is lined by a relatively thin epidermis (e). Blood channels are formed by tall pillar cells (p) that extend from either side to form strong junctional structures in the middle. The lamella is divided into two by the presence of an intralamellar septum of connective tissue (is), which splits the afferent circulation into two layers. h, haemolymph. (F) Scanning electron micrograph of a corrosion cast of the gill vasculature of *Coenobita perlatus* (cross-sectional view). A large dorsal afferent vessel (av) supplies haemolymph to each lamella via a number of afferent channels (ac) that branch extensively throughout the lamellae. A marginal canal (mc) collects the haemolymph and delivers it to the efferent vessel (ev). A few smaller efferent channels (ec) feed into the upper, medial regions of the efferent vessel. (G) Scanning electron micrograph of a corrosion cast of the gill vasculature in *Coenobita rugosus*. Dorsal view of incomplete cast of gill, showing the two vascular layers in each lamella (arrows), (separated in vivo by the intralamellar septum). av, afferent vessel; mc, marginal canal. (H–I) Light micrographs of epoxy sections through branchiostegites, stained with methylene blue. (H) *Coenobita rugosus*: The outer cuticle (cc) is thick and calcified and lined by a thick hypodermis (hd), while the inner respiratory cuticle (c) is extremely thin and uncalcified. Long, thin connective tissue partitions (ct) extend down to the respiratory surface to form the walls of the blood channels. h, haemolymph. (I) *Coenobita brevimanus*: The outer calcified cuticle has been removed (arrows). Small arteries (a) and rosette type glands (g) are present in and below the hypodermal layer. h, haemolymph. (J) Transmission electron micrograph of epoxy section through branchiostegites of *Coenobita rugosus*: The thin, inner respiratory cuticle (c) is lined by extremely attenuated extensions of the epidermis (e). The epidermal cell body lies at an acute angle to the cuticle and is attached by a long neck region, filled with microtubules (mt). Basally, the epidermal cell body contains a large nucleus (n) and joins with connective tissue cells (ct) forming the walls of the blood channels. Various haemocytes (hc) can also be observed in the blood channels. h, haemolymph.

little or no shaft structure evident, leaving a total of 10 functional gill pairs. Gills 5–7 are small, 8, 9, 10 and 12 are of medium size, and gills 11, 13 and 14 are large. In profile, the lamellae are rounded to ovate (Fig. 2(A)), with a slightly dilated marginal canal and a single nodule on the dorso-lateral margin that maintains the regular spacing between the lamellae (Fig. 2(A) and (B)). In *Birgus*, the ventral shaft of the gills is densely covered with hairs that may reach up to 1 mm in length (Fig. 2(A) and (B)). The hairs completely surround the ventral half of the gills, with a few extending up to the tops of the lamellae. They are 'wheat-like' in appearance with a long smooth, cylindrical shaft and a head formed from multiple rows of elongated, toothed scales that ring the shaft (Fig. 2(C) and (D)). These specialized hairs are not present on the gills of *Coenobita*. In contrast, the ventral gill shaft in *Coenobita* is almost bare, with only a sparse line of short, smooth, tapered spines.

3.2.2. Histology

A lamella from gill 12 of *Coenobita perlatus* was examined by light microscopy. The lamella was covered by cuticle (2 μm thick) and was lined by a relatively thin epidermis (2.6 μm thick) (Fig. 2(E)). Tall, slender epidermal cells or pillar cells extended from each side of the cuticle into the middle of the lamella where they formed strong junctions (Fig. 2(E)). Discontinuous lines of these cells radiate out across the lamella to form interconnected channels. A fenestrated layer of spongy connective tissue, supported by pillar cells extended through the middle of each lamella (Fig. 2(E)) and split the blood flowing through the lamellae into two layers.

3.2.3. Vasculature

The arrangements for the supply of blood to and from the gills are similar to those of brachyurans (Borradaile, 1903; McLaughlin, 1980). From the infrabranchial sinuses, afferent branchial vessels supply blood to the gills, whilst efferent branchial vessels carry post-branchial blood to the pericardial sinus and the heart via several large branchio-pericardial veins. The infrabranchial sinuses are supplied anteriorly by the sternal sinus and posteriorly by a pair of efferent abdominal veins that flow directly into the afferent vessel of the posterior gills. The lamellar circulation is also very similar to that of terrestrial brachyurans (Farrelly and Greenaway, 1992). Each lamella is supplied with haemolymph from a large, dorsal afferent vessel (circular in cross section) that branches profusely into smaller and smaller afferent channels that fan out across the lamella (Fig. 2(F)). This afferent network is split internally by the intralamellar septum, to form two parallel layers of interconnected blood channels (Fig. 2(G)). The bulk of the efferent blood collects in the marginal canal, which steadily increases in diameter from the dorsal to ventral surface of the lamella as it receives more and more blood (Fig. 2(F)). The marginal canals empty into the base of the large ventrally positioned efferent vessel (Fig. 2(F)). In cross-section, this efferent branchial vessel is triangular shaped and along its lateral edges there is some differentiation of blood channels into larger efferent channels that collect blood from the innermost afferent channels and flow directly into the efferent branchial vessel (Fig. 2(F)).

3.3. Branchiostegal lung

3.3.1. Coenobita

3.3.1.1. Histology. The branchial chambers are formed from vascularized outgrowths of the carapace (branchiostegites). The external surface is lightly calcified, whilst the internal (respiratory) surface is covered with a thin, transparent cuticle (Fig. 2(H)). The structures of the branchiostegal lungs were similar in the three species of *Coenobita* examined and the respiratory surface was smooth, and lacked amplification. The thick outer cuticle is lined by a well-developed epidermis below which is a layer of connective tissue containing many rosette-type glands (filled with large, rounded granules) and profiles of small arteries (Fig. 2(I)). Most of the remaining tissue in the branchiostegites is vascular and consists of large haemolymph filled sinuses, bound by connective tissue. These either extend down to the inner cuticle to form junctions with the epithelium lining the respiratory surface, or terminate just short of the respiratory membrane to form connecting exchange lacunae. A basal lamina (20–30 nm thick) lines both the epithelium and the connective tissue forming the vessel walls. The cuticle facing the lung lumen is thin (600 nm) and the epithelium lining this cuticle is extremely thin (60 nm). Consequently, the blood gas diffusion distance is very short ($\sim$700 nm). The extreme attenuation of the respiratory epithelium is achieved by confining the major cell organelles to a narrow neck region (filled with microtubules) and an expanded basal region (containing the nucleus) that joins with the adjacent connective tissue (Fig. 2(J)). Apically, thin lateral processes that lack organelles, are flattened against the cuticle (Fig. 2(J)). Such an arrangement minimizes the area of contact of the cell body with the respiratory cuticle and maximizes the area of contact of the thin lateral processes of the epidermis, thus increasing the area of lung that has short blood/gas diffusion distances. The long bundles of microtubules present in the neck of the epidermis anchor the vessel walls to the cuticle (Fig. 2(J)). Rods of electron-dense material are also deposited along the ends of the microtubules, further reinforcing the attachment to the respiratory cuticle. Bundles of muscle fibres also periodically traverse the vessel network, anchoring the two cuticles together.

3.3.1.2. Vasculature. The branchiostegal circulation is supplied anteriorly by sinuses from the head region and those that surround the stomach. A large curving sinus on each side of the cephalothorax carries venous haemolymph

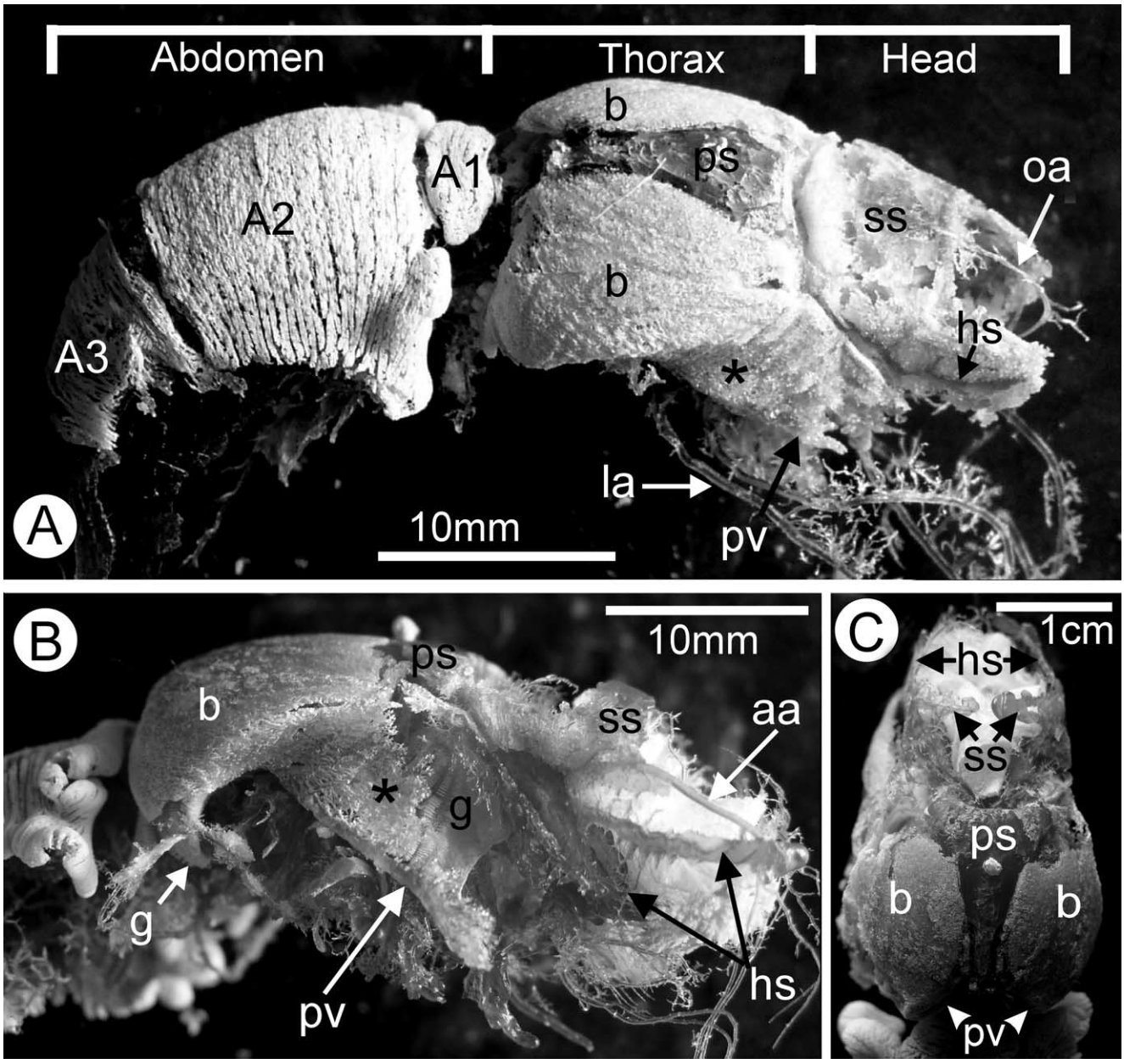

Fig. 3. (A–C) Corrosion casts of the vasculature of (A) *Coenobita rugosus* and (B–C) *Coenobita perlatus*. (A) Dorso-lateral view of full body cast; (B) lateral view of head and thoracic regions; (C) dorsal view of head and thoracic regions. A long curving head sinus (hs) runs laterally along both sides of the head, collecting venous blood from the antennal and mouthpart regions and from around the stomach (ss) to supply haemolymph to the dorsal branchiostegal regions (b). A smaller more ventral sinus arises anteriorly and runs below the cervical groove, supplying the antero-lateral regions of the branchiostegites (*) that house the scaphognathites. Oxygenated haemolymph is collected by the pulmonary vein (pv), which arises anteriorly and runs along the ventral margin of the branchiostegites, before turning medially to enter the pericardial sinus (ps). Note the gills (g) protruding posteriorly from the branchial chambers. (A1, A2 and A3) show the vascular networks in abdominal segments 1 (pedicel), 2 and 3 respectively. aa, antennal artery; la, leg arteries; oa, ophthalmic artery.

from around the antennal glands and mouthparts to the antero-dorsal margins of the lung where it joins blood originating from the stomach sinuses (Fig. 3(A) and (B)). A smaller ventral sinus supplies the anterior portions of the branchiostegite, (running below the cervical groove) and eventually unites with the larger dorsal sinus to feed into the inner dorsal margin of the lung (Fig. 3(B) and (C)).

Casts of the branchiostegal vasculature of *Coenobita* reveal dense vascularization with hundreds of branching portal vessels that interdigitate closely together (Fig. 4(A) and (B)). The lung vessels in *C. brevimanus* are short and tightly packed (Fig. 4(A)), while those of *C. perlatus* and *C. rugosus* are longer and more highly branched (Fig. 4(B)). These large vessels, which lie directly below the epidermis lining the carapace, branch towards the inner lung surface (Fig. 4(C)) where they form flattened exchange lacunae that connect the terminal branches of adjoining vessels (Fig. 4(D)). Haemolymph passes from one portal vessel into

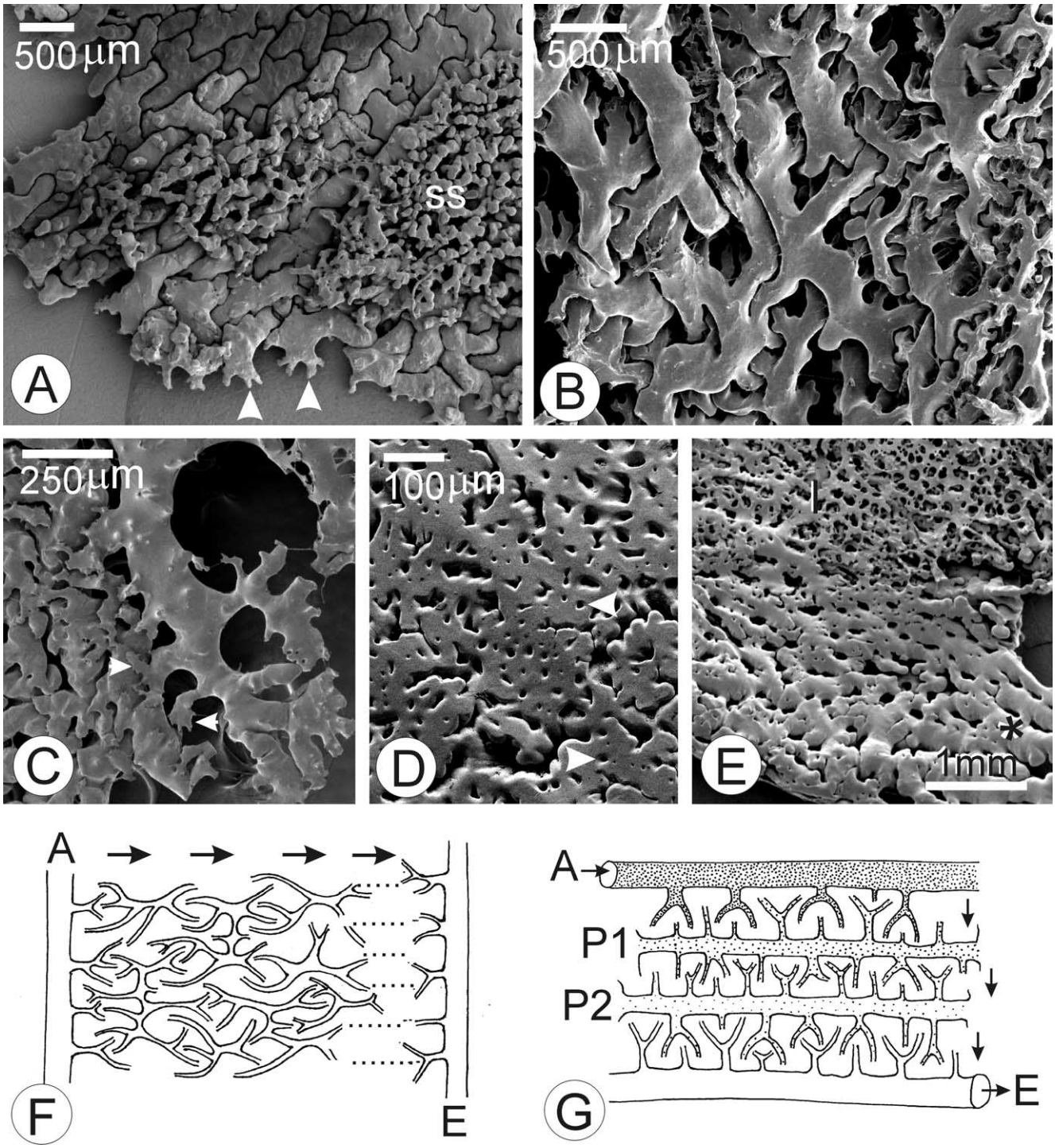

Fig. 4. (A–E) Scanning electron micrographs of vascular casts of the branchiostegal circulations. (A) *Coenobita brevimanus*, viewed from the outer surface. Short stumpy vessels interdigitate closely together; branches at either end (arrowed) extend down to the respiratory surface, where adjacent vessels are connected by lacunae, to form a series of portal vessels. A network of tiny sinuses (ss) embedded in the hypodermis overlay the pulmonary vessels. (B) *Coenobita perlatus*, viewed from outer surface. Branchiostegal vessels are highly branched and interdigitate together to form a series of portal vessels connected by lacunae. (C) *Coenobita perlatus*, viewed from the lumen side of the branchial chamber. The ends of each vessel extend down to the respiratory surface, where they terminate in flattened lacunae (arrows). (D–E) *Coenobita brevimanus*, viewed from the lumen side. (D) Flattened lacunae border the respiratory surface of the lung. Small holes in lacunae (arrows) indicate the positions of epithelial cell bodies. (E) Shows the transition of vessels from the anterior region of the branchiostegites covering the scaphognathites, where vessels form a single layer (*), to the branchial region forming the lung, where a layer of thin lacunae (l) borders the respiratory surface. (F) Diagrammatic model of the vascular organization in the branchiostegal lungs of *Coenobita*. Haemolymph passes from the afferent vessels (A), through a series of smaller interdigitating vessels and then into the efferent vessels (E). Each vessel functions as a single portal vessel and (except those along the afferent and efferent margins of the branchiostegites) begins and terminates in a lacuna (represented by

the interdigitating branches of another portal vessel via the lacunae that line the respiratory membrane and since there are many individual vessels, haemolymph passes through multiple lacunae in its passage across the lung, as illustrated schematically in Fig. 4(F). This system is somewhat similar to the 'portal' lungs of some air-breathing brachyurans (Fig. 4(G)). Haemolymph from each lung is finally collected by a pulmonary vein that arises as a small vessel at the anterior margin of each branchiostegite (Fig. 3(A) and (B)). Each pulmonary vein increases in size as it passes around the ventral margin of the branchiostegite, before it turns medially at the posterior edge and runs forward to the pericardial cavity (Fig. 3(C)).

In contrast to the vasculature in the lining of the branchial chamber, casts of the vasculature of the anterior portion of the branchiostegites that enclose the scaphognathites, reveal a single layer of large vessels, without any secondary branching to the inner cuticle (Fig. 4(E)). Thus, in this region there is no development of exchange lacunae.

Viewed from the outer surface, the branchiostegal vasculature reveals a dense network of tiny sinuses that almost completely cover the main lung vessels (Fig. 4(A)). These sinuses are scattered throughout the epidermis and presumably supply this tissue and the outer thick cuticle with nutrients and hormones.

3.3.1.3. Surface area of branchiostegal lung. The surface areas of the branchiostegal lungs of *Coenobita* were measured from casts and thus the number of available specimens for each species was limited. The lung area of *C. rugosus* (carapace length 24 mm) was 400 mm^2 ($N=1$). *C. perlatus* (average carapace length 34 mm) had a branchiostegal area of 626 ± 71 mm^2 ($N=5$) and *C. brevimanus,* (average carapace length 38 mm) had a surface area of 888 ± 181 mm^2 ($N=2$).

3.3.2. Birgus

3.3.2.1. Histology. The branchiostegal lining of the main lung chamber in *Birgus* is greatly amplified by the evagination of the respiratory surface into small, branched respiratory lobes (Figs. 1(A) and 5(A)). The outer cuticle of the branchiostegites is very thick and calcified and is lined by a thick epidermis, which is underlaid by a layer of vesicular connective tissue, containing glands, arteries and nerves (Fig. 5(A)–(C)). Periodically, bands of striated muscle extend between the inner and outer cuticles and strongly anchor the two together (Fig. 5(B)). Large glands filled with secretory granules are present in both the epidermis (Fig. 5(B)) and at the lung surface (Fig. 5(D)). Beneath the epidermis lie numerous large blood vessels, bound by connective tissue, which branch down into the respiratory lobes (Fig. 5(A)). These vessels branch into smaller and smaller sinuses, separated only by slender strands of connective tissue, and finally open into tiny lacunae directly above the respiratory epithelium (Fig. 5(A), (D) and (E)). Storch and Welsch (1984) have described the fine structure of the lung tissue in some detail and its structure is very similar to that found in the lungs of *Coenobita* and in terrestrial brachyurans (Farrelly and Greenaway, 1993).

3.3.2.2. Vasculature. The venous blood supply to the branchiostegal lungs is similar to that described above for *Coenobita* and originates from sinuses in the head region (mouthparts, antennal glands) and surrounding the stomach. These run laterally along the head and open into afferent vessels along the anterior and dorsal margins of the branchiostegites (Fig. 6(A)). The arrangements of the outer branchiostegal vessels in the dorsal lung chamber are superficially very similar to those of *Coenobita*, and comprise multiple branching vessels that closely interdigitate, and which run in series across the lung just beneath the carapace (Fig. 6(B)). The infolded portions of the branchiostegites that form the floor of the lungs are also densely vascularized (Fig. 6(C) and (D)), with anastomosing vessels packed very closely together (Fig. 6(E) and (F)). However, the respiratory surface in *Birgus* has been extended three-dimensionally through the development of the respiratory lobes. These branchiostegal vessels, therefore, send afferent branches down into the respiratory lobes (Fig. 6(G)) where they branch into progressively smaller channels, until finally opening into thin lacunae at the respiratory membrane (Fig. 6(G) and (H)). Efferent channels then carry the haemolymph back up each respiratory lobe and into the next large vessel. Haemolymph in the lung flows through a series of these three-dimensional vessel systems, joined by thin exchange lacunae that line the respiratory lobes, and thus passes through multiple lacunal systems before reaching the pericardial cavity. Efferent haemolymph is collected from this network by the two pulmonary veins (Fig. 7(A)), which arise anteriorly and run posteriorly along the lower margin of each branchiostegite (Fig. 7(B)). At the posterior margin of the lung they turn medially and run forward on either side of the pericardial sinus (Fig. 6(B)) before moving deeper to join the pericardial cavity. Just before entering the pericardial cavity, each pulmonary vein joins the branchiopericardial veins returning haemolymph from the gills on that side of the body.

space between vessels). Thus haemolymph passes through numerous lacunae in its passage across the lung. Dotted lines indicate the presence of many more vessels and lacunae than if shown. Arrows indicate direction of blood flow. (G) Diagrammatic model of the vascular organization in the branchiostegal lungs of terrestrial grapsoid brachyurans. Afferent (A) and efferent (E) systems are separated by two 'portal' systems (P1 and P2), where each portal system is formed from a single, large anastomosing vessel. Each of these portal vessels begins and ends in a lacuna, and therefore the number of lacunae between the afferent and efferent systems is fixed at three. Space between vessels represents a single lacunar bed. Arrows indicate direction of blood flow.

The flexible ventral portions of the branchiostegites, that cover the gills and the anterior portion that houses the scaphognathites, have smooth linings and lack the branched respiratory lobes present in the main lung chamber. Here, the vasculature is similar to that of *Coenobita*, with interdigitating afferent and efferent branchiostegal vessels joined by small, flattened exchange lacunae that line the respiratory surface (Fig. 7(C)). The most anterior branchiostegal vasculature comprises a single layer of large vessels, with no lacunal network.

As in *Coenobita*, the outer surface (carapace side) of the branchiostegal vasculature is covered with a dense network of small sinuses that almost completely cover the main branchiostegal vessels (Fig. 7(B)).

3.4. The abdominal lung

3.4.1. External morphology

The abdomen of *Coenobita* is connected to the thorax by a narrow pedicel (the first abdominal segment) (Fig. 1(D) and (E)). Apart from a narrow transverse ridge, on each of the first five abdominal segments and a broader plate on the sixth segment and telson that are the remnants of the tergites (Fig. 1(D) and (E)), the abdomen is covered with a thin, transparent, flexible cuticle. A more opaque patch of integument extends along the dorsal surface of the abdomen from the midline to mid-lateral zones, where the surface is folded into hundreds of tiny grooves that run transversely across the abdomen (Fig. 1(A)–(D)). These grooves enclose narrow air spaces with a large surface area and function as respiratory air-sacs. The patches are strongly vascularized and their distribution varies between species. In *C. perlatus* and *C. rugosus* they are present in abdominal segments 1 (pedicel), 2 and 3 (Fig. 1(B), (C) and (E)), whilst in the more terrestrial *C. brevimanus*, the vascular patches occur in segments 1–5 (Fig. 1(A) and (D)). Two large contractile pouches are situated ventro-laterally, one on either side of the second segment of the abdomen (Fig. 1(C) and (D)).

3.4.2. Histology

The abdominal respiratory networks of each species share a similar general architecture with an outer vascular layer overlying a thick band of striated muscle that encircles the abdomen and encloses the extensive midgut gland (Fig. 8(A)). Numerous venous sinuses surrounded by connective tissue open into flattened exchange lacunae that line the lateral walls and tips of the respiratory grooves (Fig. 8(B)). These lacunae drain into large efferent blood vessels that lie below the bases of the respiratory grooves (Fig. 8(A) and (C)). Haemolymph from the lacunae of many neighbouring grooves is collected by a single vessel (Fig. 8(C)).

The closely pleated grooves that form the invaginated air-sacs in the respiratory patches are 45–50 μm deep and 10 μm wide and many have small branches at their base that serve to further increase the surface area for gas exchange (Fig. 8(D)). In contrast, the folds in the non-respiratory part of the dorsal integument are very widely spaced (Fig. 8(E)). Rosette-type glands, similar to those found in the branchiostegites are also often associated with the bases of the respiratory grooves (Fig. 8(D)). Sensory hairs also occur intermittently across the dorsal integument (Fig. 8(D)).

The cuticle covering the dorsal surface of the abdominal lung and lining the lateral walls of the air sacs is very thin (100–250 nm) (Fig. 9(A) and (B)). The epithelium that lines this cuticle is also very thin (30–60 nm) and is coated by a basal lamina 20–30 nm that lines the vascular space (Fig. 9(B)). Thus the total blood/gas diffusion distance is 200–350 nm. As in the branchiostegal lungs, the epithelium is highly attenuated with extended lateral processes that are flattened against the cuticle to form a thin sheet, while the epithelial cell body containing the nucleus and other organelles is restricted to a narrow neck that projects into the underlying haemocoel (Fig. 9(A) and (B)). Apically it is anchored to the cuticle by rods of electron dense material (Fig. 9(B)). Basally, the epithelial cell body joins with connective tissue forming the vessel walls (Fig. 9(B)). The perikaryal basal membrane of the epithelial cells is highly folded, and forms long thin processes that interdigitate closely with neighbouring cells (Fig. 9(A)). The function of these intricately arranged folds is unknown. Pillar cells (Fig. 9(C)) filled with long microtubules occur in areas of mechanical stress and strongly anchor the vessel walls to the cuticle. Small arteries and nerves are also present near the base of the respiratory grooves (Fig. 9(D)).

Integumental tissue from the posterior, non-respiratory part of the dorsal abdomen of *C. perlatus* was also examined for comparison, and in this region the cuticle measured 4 μm, 16× thicker than that covering the respiratory patches (Fig. 8(E)). The surface was periodically invaginated but did not have the regular, closely pleated grooves that occur across the surface in the respiratory patches. The cuticle was lined by a tall, columnar epithelium (~16 μm thick) (320× thicker than that lining the respiratory patches) (Fig. 8(E)), underlain by a dense layer of connective tissue containing numerous glands. Below this was a thick layer of striated muscle (Fig. 8(E)). There was no vascular layer at all in this region and clearly no respiratory network was present in this part of the integument.

3.4.3. Surface area of abdominal lung

The respiratory grooves occur on the dorsal abdomen at a frequency of 300 cm^{-1} and are approximately 50 μm deep and 33 μm apart. Gas exchange is likely to occur primarily via the two lateral walls of each side of the groove and on the dorsal surface between each groove. In *C. rugosus* (carapace length of 24 mm), where the abdominal lung is comprised of three abdominal segments, the estimated surface area of the respiratory grooves was 1864 mm^2 ($N=1$). *C. perlatus*, (mean carapace length, 34 mm) also with three abdominal lung segments, had an abdominal lung area of 2361 ± 138 mm^2 ($N=5$), whilst in *C. brevimanus,* (mean

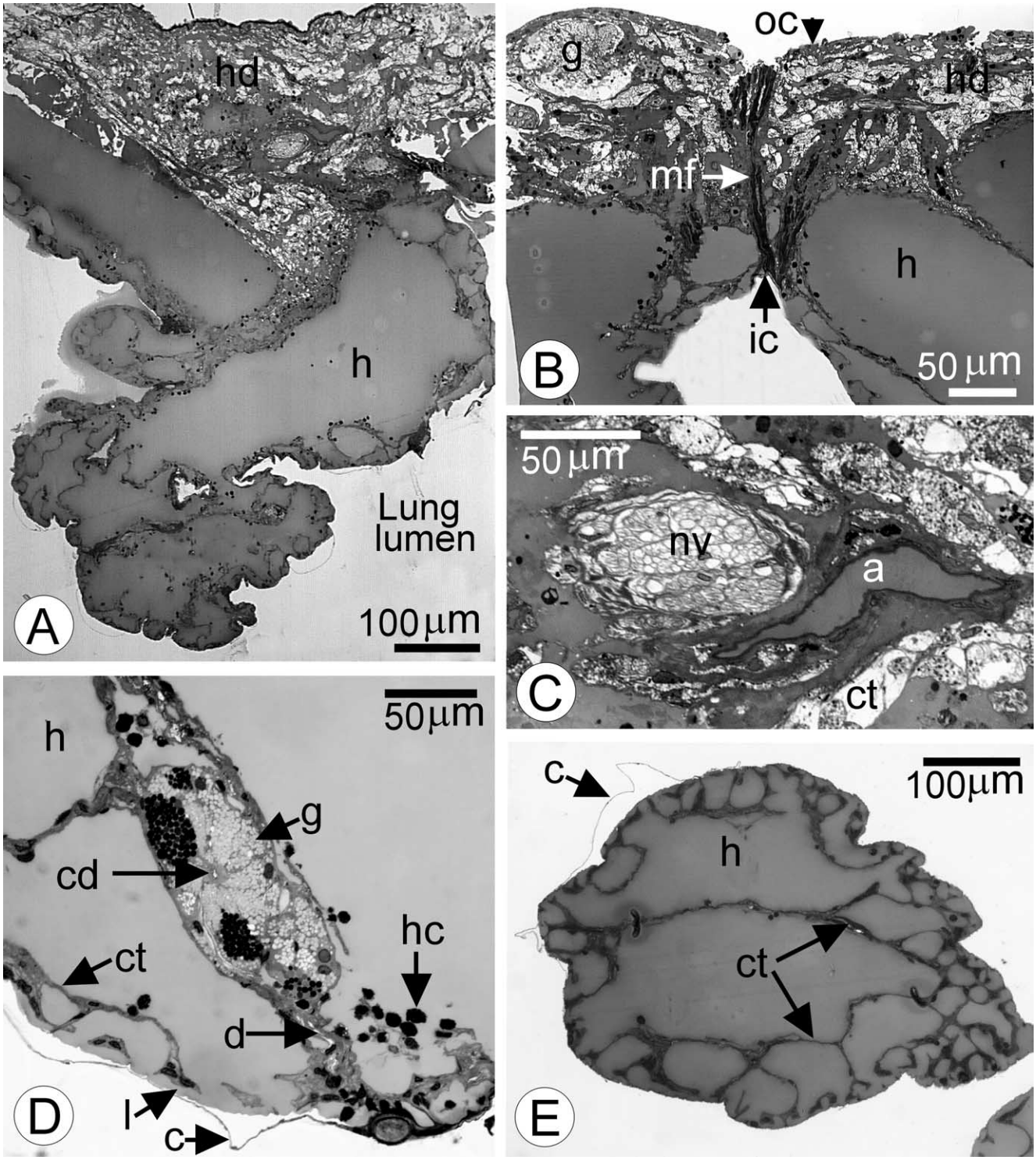

Fig. 5. (A–E) Light micrographs of epoxy sections through the branchiostegal lung of *Birgus latro* (outer calcified cuticle has been removed). (A) Cross-section through branchiostegite showing the elaborately branched lobes of the lung. Below the calcified cuticle lies a thick hypodermis (hd) and a layer of connective tissue containing small sinuses, arteries, nerves and glands. Below this lie the pulmonary vessels that extend down into the respiratory lobes. h, haemolymph. (B) Between respiratory lobes, the lung tissue is strongly anchored to the outer calcified cuticle by muscle fibres (mf), which stretch from the outer calcified cuticle (oc) (removed), through the hypodermis (hd) to the inner cuticle (ic). g, rosette gland; h, haemolymph. (C) Enlargement of section through hypodermis showing profile of nerve bundle (nv) and an artery (a), surrounded by haemolymph in small sinuses. ct, connective tissue. (D) Longitudinal section through lung lobe showing a large gland complex (g), secreting its product through a narrow duct (d) directly onto the respiratory surface. Note that the respiratory cuticle (c) has partially pulled away from the rest of the lung tissue. cd, central duct of gland; ct, connective tissue; h, haemolymph; hc, haemocytes; l, lacunae. (E) Cross-section of single lung lobe. Blood vessels are separated by thin partitions of connective tissue (ct) and branch into successively smaller and smaller sinuses until they open directly onto the epithelium lining the respiratory cuticle (c) (partially pulled away). h, haemolymph.

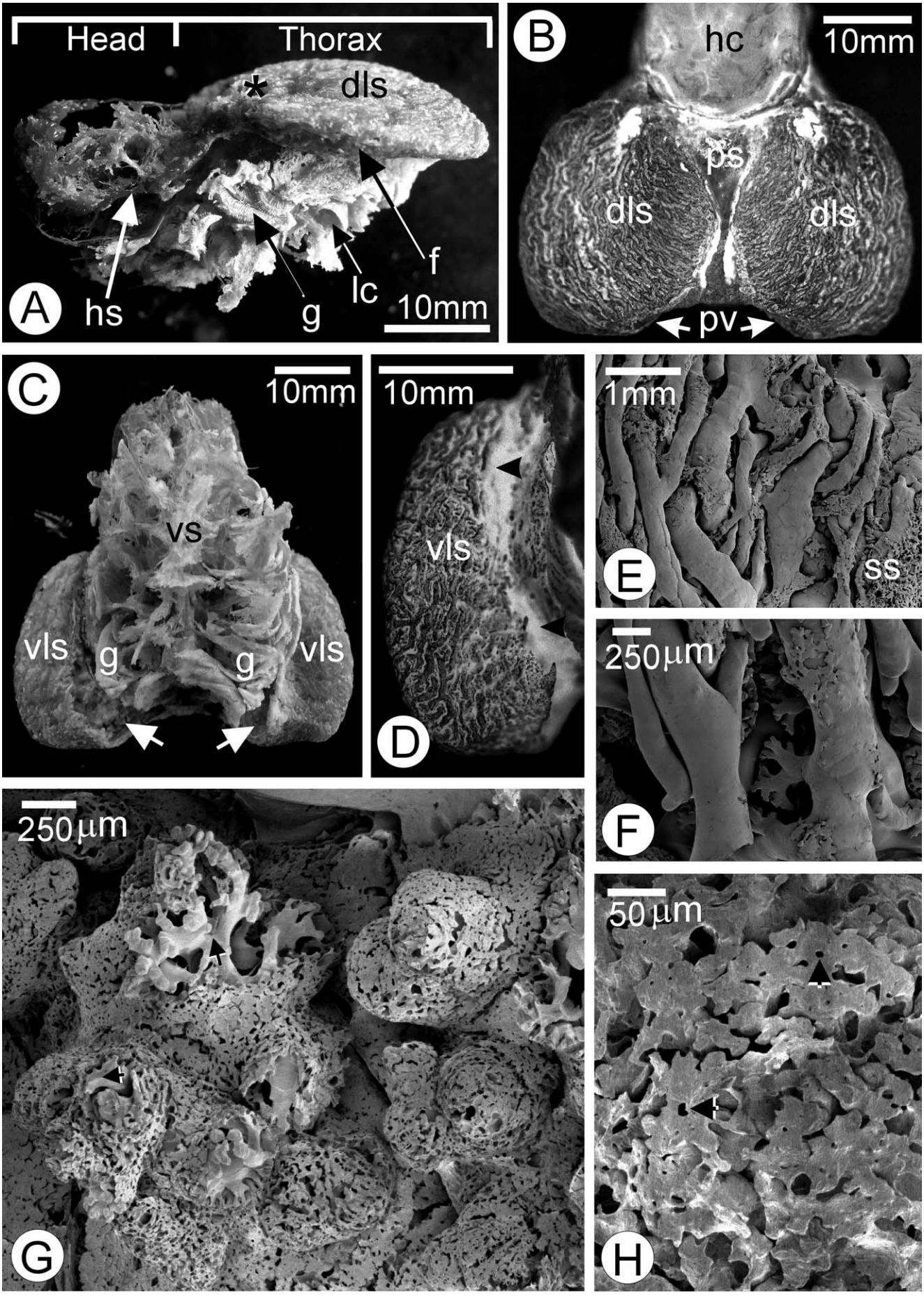
Head
Thorax
dls
hs
g
lc
f
10mm
A
B
hc
10mm
ps
dls
dls
pv
C
10mm
vs
vls
g
g
vls
D
10mm
vls
E
1mm
ss
F
250μm
G
250μm
H
50μm

carapace length, 38 mm) with five abdominal lung segments, the respiratory grooves had a surface area of 5936 ± 284 mm^2 (N = 5). For each species, the individuals were of a narrow size range but unfortunately only carapace lengths were measured. In the absence of body mass data, weight specific surface areas could not be calculated. These figures probably underestimate the total surface area available for gas exchange as many of the air-channels had small side branches.

3.4.4. Vasculature

From the corrosion casts, it is evident that a large vascular network is present on the dorsal surface of the abdomen of the three species of *Coenobita* studied (Figs. 3(A) and 10(A)) and in *Birgus* (Fig. 10(B)). This network is supplied from the thorax by two large afferent vessels (afferent abdominal veins) that extend from each side of the ventral (sternal) sinus and run dorsally down either side of the abdomen (Fig. 10(B) and (C)), and by a number of smaller channels that run between and parallel to these two large outer vessels (Fig. 10(D)). These smaller channels arise from the large dorsal sinus in the abdomen and branch laterally on either side to form a network of afferent cross-channels that traverse the abdomen (Fig. 10(D)). Small sinuses from these branch upwards (Fig. 11(A)), feeding into the exchange lacunae lining the air sacs (Fig. 11(B)). Returning haemolymph is collected by rows of tiny 'T-shaped' efferent channels joined at their ends (Fig. 11(C)–(E)), which branch back down into a well-developed system of anastomosing efferent cross-vessels that flow into large efferent veins either side (Figs. 10(A), 11(F) and (G)). The connections between adjacent 'Ts' appear quite constricted (Fig. 11(D) and (E)) and this may increase resistance between 'Ts', thus channelling haemolymph down the central part of the 'T' and into the efferent vessel below. The efferent cross-channels are large and rounded in cross-section, with smooth undersides (Fig. 11(E) and (G)) and lie above the afferent cross-channels, which are relatively flattened in cross-section (Fig. 11(A)). This network is illustrated schematically in Fig. 12(A) and (B).

The paired efferent abdominal veins drain haemolymph from the dorsal network and then flow forward into the thorax where they directly connect with the afferent vessel that supplies the last four gills on each side (arthrobranchs and pleurobranchs of limbs four and five) (Fig. 12(C)). This pattern is the same in each species, including *Birgus* (Figs. 10(B) and 12(D)). Haemolymph from the abdominal network is therefore returned to the pericardial cavity via the gills and the branchiopericardial veins, i.e. there is no direct return of haemolymph from the abdomen to the pericardial cavity. The abdominal lung thus functions in series with the gills, as illustrated by the schematic model shown in Fig. 12(E).

It is clear from the casts that the abdominal circulation of *Birgus* is similar to that of other coenobitids with paired afferent and efferent abdominal veins on each side connected by a distinct vascular network (Fig. 10(B)).

4. Discussion

4.1. Gills

Air-breathing coenobitids have a similar number of gills as the aquatic Paguridae and aquatic and intertidal Diogenidae (14, 9–13 and 13–14 pairs, respectively) (Davie, 2002). However, comparison of the number of gill lamellae on each gill indicates that gill mass has been significantly reduced in the coenobitids compared to the pagurid hermit crabs (Harms, 1932) with most of that change being due to the extreme reduction of the anterior gills. In *Coenobita,* only the last 10 pairs of gills are of a functional size. The gill lamellae in the pagurids are relatively long and ovate (Harms, 1932) but in the coenobitids the lamellae are small and rounded and have a markedly reduced surface area (Greenaway, 1999). The weight specific gill area of *Birgus* (mm^2) = 152.1 (body mass in grams)$^{0.686}$ and that of *Coenobita* is of the same order (Greenaway, 1999, 2003), which compares with the most extreme reduction of gill area seen in air-breathing brachyurans (Greenaway, 1999). This undoubtedly reflects a decreased dependence on the gills for gas exchange and the development of other respiratory surfaces.

The cuticle of the gill lamellae of air-breathing brachyurans is generally much thicker than in their aquatic relatives (Taylor and Taylor, 1992) and this provides necessary rigidity and support for the lamellae in the lower density of air. A similar difference is evident between

Fig. 6. Corrosion casts of the vasculature of *Birgus latro*, showing the branchiostegal circulation (abdomen removed). (A) Lateral view, showing the large, lateral running head sinus (hs) that supplies the afferent vessels of the lung (*). f, branchiostegal fold; dls, dorsal lung surface; g, gills; lc, leg coxae. (B) Dorsal view showing densely vascularized branchiostegites; the carapace covering the head (hc) has not been removed. dls, dorsal lung surface; ps, pericardial sinus; pv, pulmonary veins. (C) Ventral view of (B), showing the fold in the ventral portion of the branchiostegite, which separates the upper, expanded lung compartment from the lower gill cavity. Gills (g) can be observed protruding from the back of the gill chamber and part of the internal lung vasculature can also be observed (arrows). The ventral sinus (vs) runs along the midline. vls, ventral lung surface. (D) Vasculature of the branchiostegal fold from an isolated lung (ventral view). The lung cavity (arrow heads) has been filled with a white fatty substance during the corrosion process. vls, ventral lung surface. (E) SEM of outer branchiostegal surface, showing the closely interdigitating pulmonary vessels. Small sinuses (ss) are embedded in the hypodermis and cover the larger pulmonary circulation. (F) SEM of outer branchiostegal surface, showing the pulmonary vessels branching down to the respiratory surface below. (G) View of vasculature supplying the respiratory lobes. Afferent branches from the outer pulmonary vessels extend into the lung lobes (arrows) where they terminate in flattened lacunae that line the respiratory surface. (H) High powered view of the respiratory lobes, showing that the respiratory surface is lined with flattened lacunae. Small holes (arrows) indicate the former position of epithelial cell bodies.

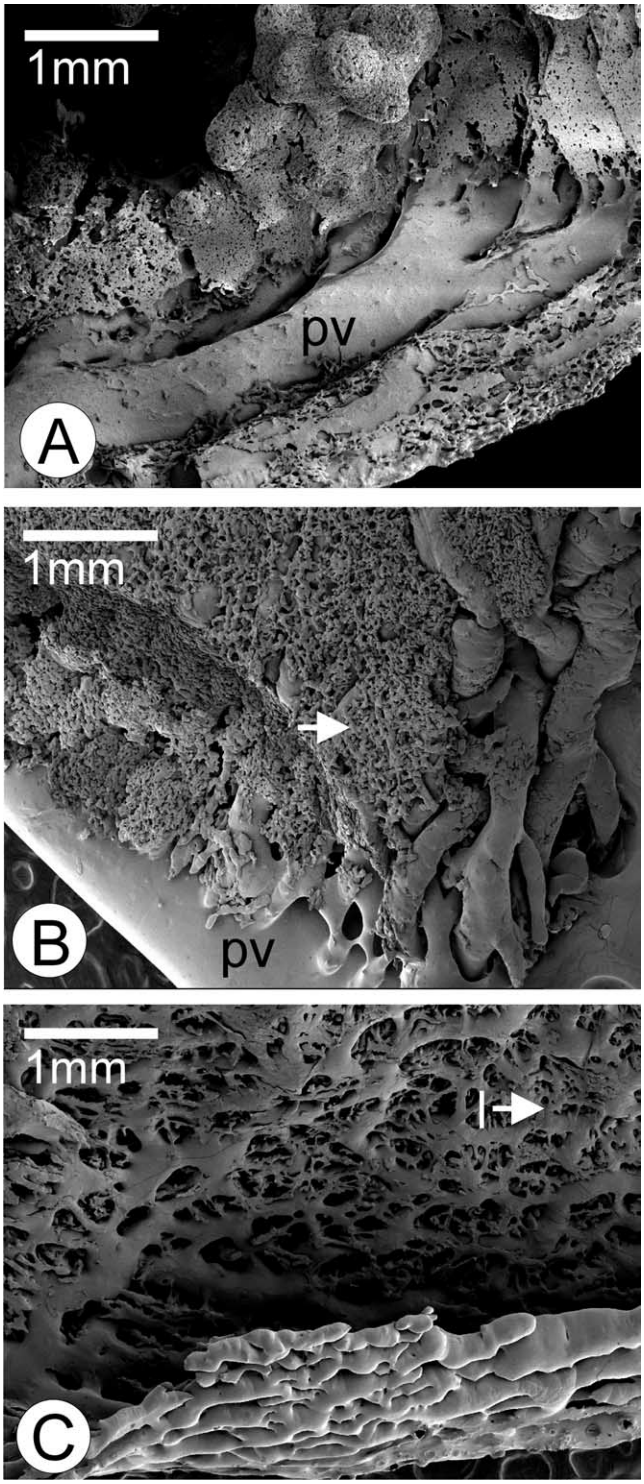

Fig. 7. Scanning electron micrographs of vascular casts of the branchiostegal vasculature of *Birgus latro*. (A) View from lumen side of lung, showing vessels from the respiratory lobes of the lung flowing into the large pulmonary vein (pv), which returns efferent blood to the pericardial sinus. (B) View of outer branchiostegal surface, showing part of the large pulmonary vein (pv) that runs around the margin of the branchiostegite. Note the small sinuses (arrow) that cover the external surface of the main pulmonary vasculature. (C) Inner view of anterior part of branchiostegite that covers the scaphognathites. Note how the branchiostegite is folded in ventrally. Here the branchiostegal lining is smooth and the vessels form a simple network, joined by small sinuses and lacunae (l).

gill cuticles of the terrestrial *C. rugosus* and the aquatic pagurid *Diogenes pugilator* (Harms, 1932). In this study, the gill cuticle of *C. perlatus* was ~2 μm thick, thicker than that of aquatic crustaceans but well within the range reported for air-breathing crabs. Additionally, the lamellae exhibited other features characteristic of the gills of air-breathing brachyurans, notably expanded marginal canals and a row of nodules to ensure regular spacing (Greenaway and Farrelly, 1984; Farrelly and Greenaway, 1987, 1992).

The histology of the gill lamellae was similar to that of the phyllobranch gills of other decapods (Taylor and Taylor, 1992). Current observations on the gill lamellae from the posterior gills of *C. perlatus* (gill 12), showed the epithelium to be ~2.4 μm thick. This is relatively thin compared to values for other air-breathing crustaceans, in which the epithelium may be as much as 10 μm in thickness (Taylor and Taylor, 1992) and this is consistent with a primary role in gas exchange. The structure of the gills of air-breathing crustaceans varies considerably depending on whether they are modified primarily for ion regulation or for gas exchange. Clearly the cellular apparatus required for ion regulation (large surface area of infolded membranes and abundant mitochondria for driving the process) results in a thickened epithelium, whereas an effective respiratory epithelium must be thin in order to minimize blood/gas diffusion distances. Gills that are primarily modified for osmoregulation will be less efficient in gas exchange. However, the development of alternative sites for gas exchange in air-breathing crustaceans has freed the gills for other functions without compromising the overall efficiency of gas exchange in the animals. Thus the pattern of gill function may vary within or between the lamellae and/or between gills, with either the anterior or posterior gills being essentially modified for ion-regulation. In *C. perlatus*, the posterior gills appeared to be primarily involved in gas exchange, whilst the gills of *C. rugosus* (examined by Harms, 1932) appear to be modified for ion regulation (however, it is not known which gills were studied by Harms). Further structural studies are needed to clearly identify the primary role of the different gills in the Coenobitidae.

As a result of early studies using ink injections, Bouvier (1890a) concluded that the lamellar circulation of the gills of *C. clypeatus* (formerly *C. diogenes*) was poorly developed. However, evidence from corrosion casting presented in this study does not support this conclusion. Indeed, the lamellae are well-perfused and the pattern of blood flow was very similar to, and just as well developed as those of both aquatic and air-breathing brachyurans (Drach, 1930; Taylor and Greenaway, 1979; Farrelly and Greenaway, 1992). Perfusion of the lamellae therefore appears to be largely unrestricted, except for possible narrowing at the boundary between the afferent and efferent channels, along the edge of the intralamellar septum. This phenomenon is also observed in the air-breathing Brachyura (Farrelly and Greenaway,

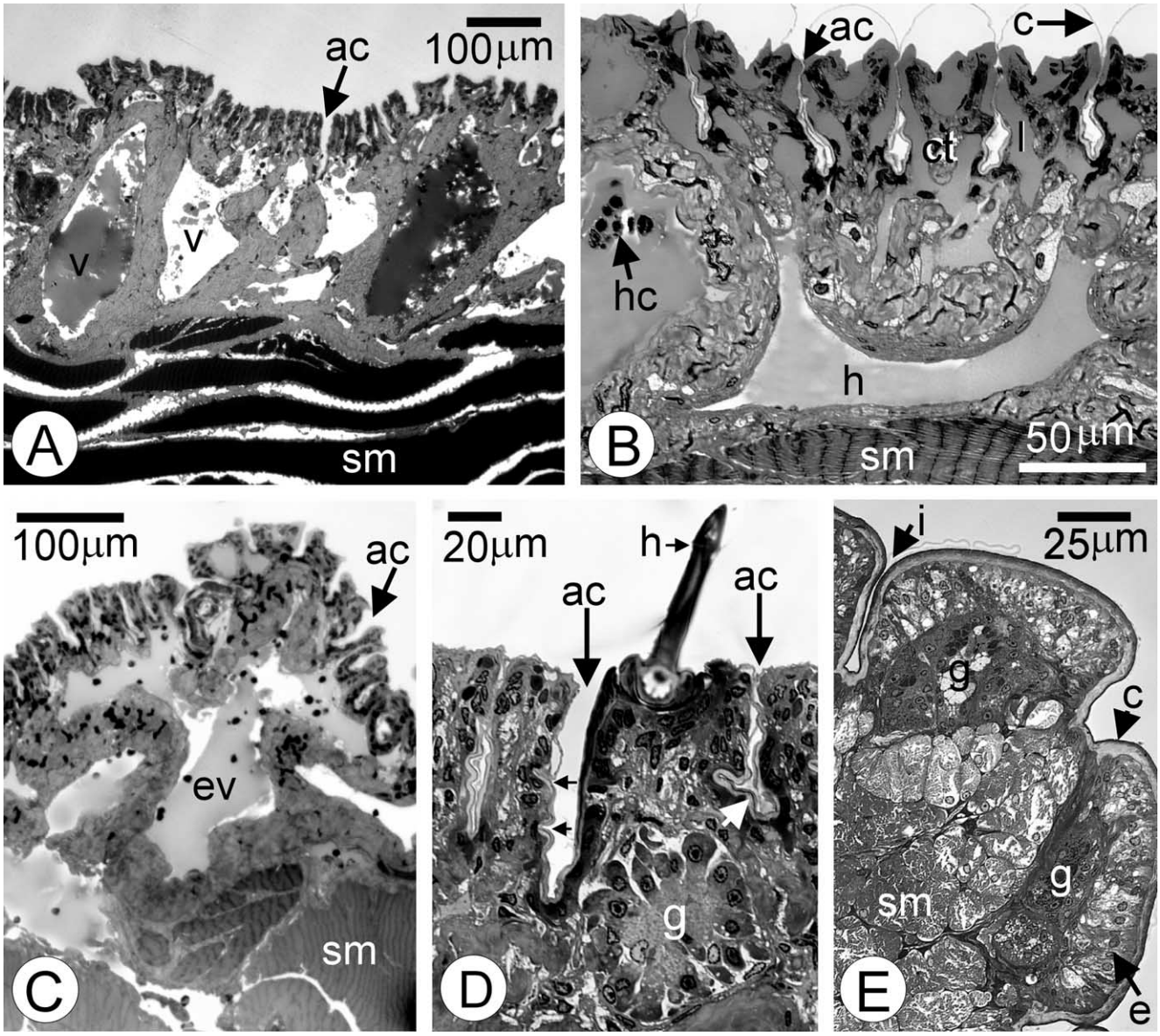

Fig. 8. (A–E) Light micrographs of epoxy sections through the dorsal abdominal integument of *Coenobita*. (A) *C. brevimanus*, low power view of longitudinal section. The dorsal surface is highly folded and forms narrow, air-filled pleated channels (ac) that run across the abdomen and which function as respiratory air-sacs. Below the respiratory grooves is a vascular layer containing large blood vessels (v), which sits upon a thick layer of striated muscle (sm). Note that haemolymph from some vessels has been lost during sectioning. (B) *C. rugosus*. High power view of a longitudinal section through the respiratory grooves, showing the air-channels (ac) and the exchange lacunae (l) that line the edges of the grooves. The lacunae are bordered apically by a very thin respiratory epithelium and cuticle (c) (which has ballooned away from parts of the tissue during preparation) and basally by connective tissue partitions (ct) that direct haemolymph back down into the efferent vessels below. h, haemolymph; hc, haemocytes; sm, striated muscle. (C) *C. brevimanus*. Longitudinal section through respiratory network, showing a cross-section of a large efferent cross-vessel (ev) with its many collecting branches that drain the rows of blood channels lining the respiratory grooves. ac, air-channels; sm, striated muscle. (D) *C. perlatus*. High power view of air-channels (ac) in respiratory grooves showing small folds along the sides and at their base (arrows) that increase their surface area. A large rosette-type gland (g) can be observed near the base of the groove and hairs (h) are also occasionally present on the outer dorsal surface. (E) *C. perlatus*. Longitudinal section through non-respiratory part of the dorsal integument. The cuticle (c) is comparatively thick and is lined by a tall, columnar epithelium (e). Large multicellular glands (g), surrounded by connective tissue lie below. And beneath this lie large bundles of striated muscle (sm). Widely spaced folds form irregular invaginations (i) across the surface.

1987, 1992), but may be an artefact of the corrosion process (see Taylor and Taylor, 1992).

The gills of the air-breathing coenobitids have a reduced surface area (fewer gills and fewer and smaller lamellae) and an increased blood/gas diffusion distance (thicker cuticle and epithelium) compared to aquatic hermit crabs and both these factors would tend to reduce the efficiency of oxygen uptake. Indeed the gills of *Birgus* are ineffective in O_2 uptake (Greenaway et al., 1988). This suggests that the gills are no longer the primary site of gas exchange, although they may still have an important role in the excretion of carbon dioxide (Greenaway et al., 1988; Morris

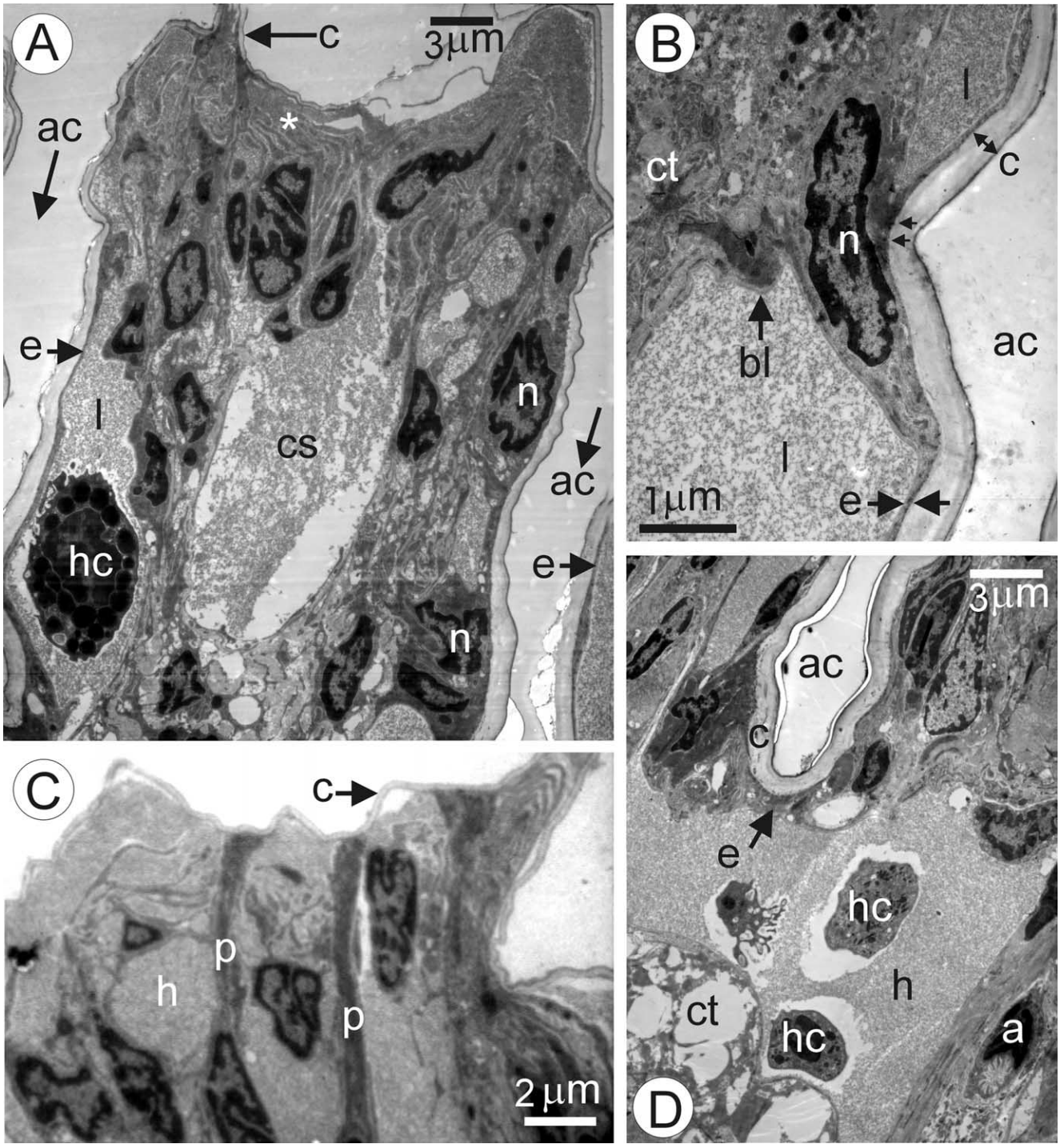

Fig. 9. Transmission electron micrographs of epoxy sections through the dorsal abdominal integument of *Coenobita brevimanus*. (A) Cross-section through abdominal lung, showing the very thin cuticle (c) and epithelium (e) lining the respiratory grooves. A central sinus (cs) can be observed that opens into lacunae (l) that line the edges of the grooves. Note the complex, highly folded baso-lateral membranes of some epithelial cells (*) and the large nucleus (n) of the epithelial cell body; ac, air-channels; hc, haemocyte. (B) Higher power view of abdominal lung showing thin cuticle (c) and epithelium (e) lining the respiratory grooves and bordered by lacunae (l). The epithelial cell body, containing a large nucleus (n), projects away from the respiratory surface and interdigitates closely with underlying connective tissue cells (ct). Apically, rods of electron dense material (arrows) anchor the epithelial cell body to the cuticle. A thin basal laminar (bl) lines the vascular space; ac, air-channel. (C) In areas of mechanical stress, epidermal cells bodies are filled with long microtubules, forming thin pillar like cells (p), which anchor the vessel walls to the cuticle (c) and prevent distension of lung walls. h, haemolymph. (D) The base of the respiratory grooves is lined by a slightly thicker cuticle (c) and epidermis (e) and is closely associated with glands, arteries (a) and nerves. ac, air-channel; ct, connective tissue cells; h, haemolymph; hc, haemocytes.

and Greenaway, 1990). Clearly, with reduced branchial function, the development of alternative respiratory sites is essential for terrestrial coenobitids.

4.2. Branchiostegal lungs

The branchial chambers of *Coenobita* are small and narrow and are occupied almost entirely by the large posterior gills and pericardial sacs, which lie directly against the branchiostegal wall and thus further reduce the surface area of the branchiostegites available for gas exchange. Additionally, the inner respiratory lining of the branchiostegites is smooth and thus the surface area available for gas exchange across the branchiostegal lung is small. Branchiostegal areas ranged from 400 mm^2 in *C. rugosus* (carapace length 24 mm) to 888 mm^2 in *C. brevimanus* (carapace length 38 mm). Although strict weight specific comparisons of surface area cannot be made, it is evident that these areas are significantly smaller than the smooth lungs of the air-breathing brachyurans *Holthuisana transversa* (Greenaway, 1984), *Discoplax hirtipes* and *Gecarcoidea natalis* (Farrelly and Greenaway, 1993).

Harms (1932) compared the structure of the branchiostegites of *C. rugosus* with those of the aquatic hermit crab *Diogenes pugilator* and found that the inner respiratory lining of the branchiostegites was 5× thinner in *C. rugosus*. Indeed, the blood/gas diffusion distance across the lung of *Coenobita* (700 nm) measured in this study is comparable with that of *Birgus* (500–1200 nm) (Storch and Welsch, 1984), and with values for air-breathing brachyurans (250–800 nm) (Farrelly and Greenaway, 1987, 1993; Storch and Welsch, 1975; Taylor and Greenaway, 1979). Clearly, the branchiostegites of *Coenobita* are modified for aerial gas exchange but to a much lesser extent than in *B. latro* where the branchial chambers are expanded and the lung surface is greatly elaborated.

4.3. Branchiostegal blood supply

Venous blood is supplied to the branchiostegites of coenobitids via sinuses around the mouthparts and antennal glands and also from sinuses surrounding the stomach. Similar supply channels are also found in air-breathing brachyurans (Greenaway and Farrelly, 1984; Farrelly and Greenaway, 1993). Casts of the branchiostegites of *Coenobita* exhibit dense vascularization with a series of closely interdigitating branched portal vessels, joined by thin lacunae bordering the respiratory membrane. Haemolymph flows from one large vessel into another via these lacunae, thus passing through numerous sets of lacunae in its passage across the lung. The pulmonary vein, which runs around the margin of the branchiostegite, collects the efferent blood and returns it to the pericardial sinus. This system resembles the lung vasculature of many smooth-lunged air-breathing brachyuran crabs (von Raben, 1934; Farrelly and Greenaway, 1993). In such crabs, there are two discrete portal systems, each formed from a single, highly branched anastomosing vessel, that lie between the afferent and efferent systems, with each system joined by lacunae, thus producing a total of three connecting lacuna beds that function in series (Fig. 4(G)). The convergent development of these 'serial lacunar systems' is consistent with some selective advantage in terms of efficiency of gas exchange. It may be that only a small percentage of the haemolymph is oxygenated in each lacunar transit and therefore many 'sweeps' are necessary to fully mix and oxygenate all the haemolymph. The maximum length of a lacuna is restricted for mechanical and structural reasons and to achieve oxygen saturation it may be necessary for the blood to pass through many tiny lacunae rather than a single set of larger ones. Such a system may be of particular importance during exercise when perfusion rates are high and where serial oxygenation may serve to ensure maximum saturation. Taylor and Taylor (1992) have suggested that countercurrent transfer of oxygen between closely packed vessels might also be reduced in serial lacunar systems, where O_2 gradients between adjacent vessels are small compared to systems comprising only afferent and efferent vessels, where gradients are large. This system would maximize oxygenation of the haemolymph.

The branchiostegal circulation in adult *Coenobita* is not a new evolutionary development but a retention and development of the branchiostegal circulation present in the larval stages, as also obtains in brachyurans (Jackson, 1913; Harms, 1929). This circulation serves as the main respiratory site in the larvae before the appearance of the gills, which then take over the main respiratory function in the later aquatic larval stages (Bouvier, 1890b; Jackson, 1913).

4.4. The abdominal lung and its blood supply

As discussed above, the branchiostegites of the coenobitids are better adapted for gas exchange than those of the pagurids. However, their gas exchange capacity is limited by their relatively small surface area and anatomically they are not as effectively organised as those of *Birgus* or some of the air-breathing brachyurans (von Raben, 1934; Greenaway and Farrelly, 1984; Farrelly and Greenaway, 1987, 1993). Although both branchiostegites and gills provide functional respiratory surfaces, their gas exchange capacity seems insufficient to sustain the total respiratory needs of the animals and this has resulted in selective pressure favouring the development of an entirely new respiratory organ: the abdominal lung. This organ was first described by Bouvier (1890a) and then later by Borradaile (1903) and Harms (1932). Much of this early work was based on pericardial injections of ink and subsequent dissection and while the basic anatomical detail reported was correct, fundamental errors of interpretation were made in regard to the anatomy of the abdominal veins and the return of haemolymph from the abdominal lung to the pericardium.

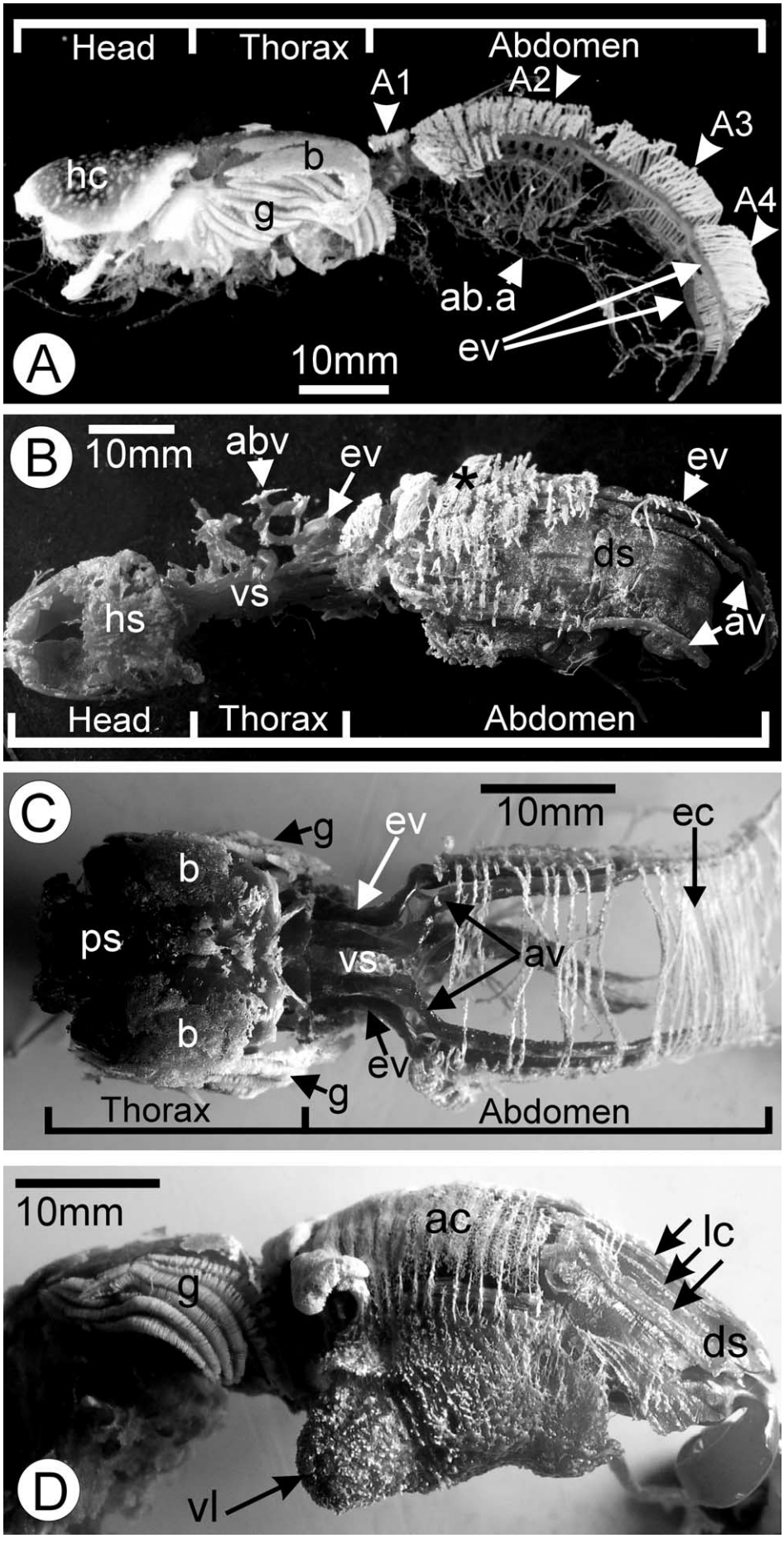
Head
Thorax
Abdomen
A1
A2
A3
A4
hc
b
g
ab.a
ev
A
10mm
B
10mm
abv
ev
*
ev
ds
vs
hs
av
Head
Thorax
Abdomen
C
g
ev
10mm
ec
b
ps
vs
av
b
ev
g
Thorax
Abdomen
10mm
ac
lc
g
ds
D
vl

The casts of the vasculature, made in this study, provide much greater detail of the abdominal network and also clarify the true relationships between the major venous sinuses, the abdominal veins and the pericardial sinus. These are summarised below.

It is clear from corrosion casts that the dense vascular network in the dorsal abdominal integument of *Coenobita* is supplied with venous blood from both the thorax and the abdomen. Blood from the thoracic ventral sinus flows posteriorly in two large afferent vessels that run down either side of the abdomen. Venous blood from the abdomen originates from the extensive dorsal abdominal sinus. Furthermore, the afferent veins, which lie on top of the dorsal abdominal sinus, join with the main abdominal sinus along their ventral edge, and thus are very closely connected. The dorsal abdominal sinus also gives rise to several long, thin channels that run parallel to the large lateral afferent vessels. These longitudinal channels branch laterally to form an afferent network of cross-channels. The afferent cross-channels feed the exchange lacunae that line the walls of the respiratory grooves. The lacunae in turn connect to an extensive efferent network of anastomosing cross-vessels that carry oxygenated blood to the outer efferent abdominal veins. These efferent veins run forward into the thorax where they supply the afferent vessel of the posterior gills on either side. Oxygenated blood from the abdomen must, therefore, pass through the posterior gills before it is returned to the pericardium via the branchiopericardial veins. Thus the abdominal lung functions in series with the gills (Fig. 12(C)–(E)) and not in parallel as reported in the earlier literature. The 'gas windows' of the air-breathing brachyuran crabs, *Scopimera* and *Dotilla*, also possess a respiratory system arranged in series with the gills (Maitland, 1986).

The organization described above differs in important aspects from that described previously. Bouvier (1890a) erroneously believed that the paired inner abdominal vessels (afferent veins) and outer abdominal vessels (efferent veins) all united together before exiting the abdomen and entering into the extreme posterior of the pericardium, i.e. Bouvier thought that all four vessels carried efferent blood from the abdominal lung directly to the pericardium. Clearly the exact origin and direction of blood flow in these vessels was difficult to discern using ink injections and once these fundamental descriptive errors were made they were perpetuated by later workers (see Borradaile, 1903; Harms, 1932).

In the Anomura and Brachyura the pericardial sinus receives input only from the paired branchiostegal pulmonary veins (primary route in larvae) and the five paired branchiopericardial veins (secondary route in larvae). There are three pericardial openings on each side as the pulmonary vein unites with the last branchiopericardial vein before opening into the pericardial cavity (Pearson, 1908; Jackson, 1913; Pike, 1947). In order to maximise circulatory and respiratory efficiency, oxygenated haemolymph from a respiratory surface should return directly to the heart and one might, therefore, expect that efferent vessels returning oxygenated blood from the abdominal lung would connect either with the branchiopericardial veins or directly with the pericardial sinus. In both aquatic anomurans and brachyurans, however, the abdominal veins open posteriorly into the infrabranchial sinuses. This established return route for venous blood from the abdomen via the gills (the main respiratory organ in aquatic crabs) preceded the development of abdominal respiratory function in *Coenobita* and has been retained. Retention of this route was probably a critical factor in alowing *Birgus* to dispense with the molluscan shell, which involved a secondary loss of abdominal lung function and enhancement of the role of the branchiostegal lungs. Clearly, in this example, where the abdomen no longer functions as a respiratory organ, direct return of venous blood from the abdomen to the pericardial sinus would seriously compromise the overall respiratory efficiency by diluting the oxygen content of haemolymph returning from the branchiostegal lungs. On the other hand, the return of venous haemolymph from the abdomen via the gills would clearly not affect overall respiratory efficiencies. Indeed, it may be significant that the posterior gills of *C. perlatus*, that receive the bulk of the abdominal output, were modified for gas exchange and not ion-regulation, and so may serve to further increase haemolymph oxygenation.

The forward flow of oxygenated blood from the abdomen to the posterior infrabranchial sinus means that blood samples from this site will contain a mixture of oxygenated and venous blood. This is of potential significance in studies of the respiratory physiology of *Coenobita* where it has been necessary to measure blood gas levels of venous

Fig. 10. (A–D) Corrosion casts of the abdominal vasculature. (A) *Coenobita brevimanus*. Lateral view of an efferent fill of the abdominal network. Note that abdominal segment five and the afferent abdominal system have not been filled. Large, paired efferent veins (ev), collect haemolymph from the abdominal networks and return it to the pericardial sinus via the gills (g). (A1–A4) abdominal segments 1–4; ab.a, abdominal arteries; b, branchiostegites; hc, head carapace. (B) *Birgus latro*. Dorsal view of a cast, which clearly shows the presence of an abdominal network in the dorsal integument. Paired afferent (av) and efferent veins (ev) (only one shown) connected by a network of cross-channels (*), run above a large dorsal abdominal sinus (ds). The efferent abdominal veins flow forwards and empty directly into the afferent branchial veins (abv) of the posterior gills. Note branchiostegal lungs have not been filled. hs, head sinuses; vs, ventral sinus. (C) *Coenobita brevimanus*. Dorsal view (head region has been removed). This cast shows the major veins that supply and drain the abdominal networks. The inner, paired afferent veins (av) emerge from either side of the ventral sinus (vs) and run down either side of the abdomen. The outer, paired efferent abdominal veins (ev) drain haemolymph from the dorsal network of efferent cross-channels (ec) and then flow forward into the thorax to supply the last 4 gills (g); b, branchiostegites; ps, pericardial sinus. (D) *Coenobita perlatus*, lateral view. Cast showing an afferent fill of the abdominal network. The dorsal abdominal sinus (ds) produces several longitudinal channels (lc) that feed into the afferent cross-channels (ac). Note large antero-lateral vascular lobes (vl) on abdomen that help supply the lateral branches of the afferent system on either side. g, gills.

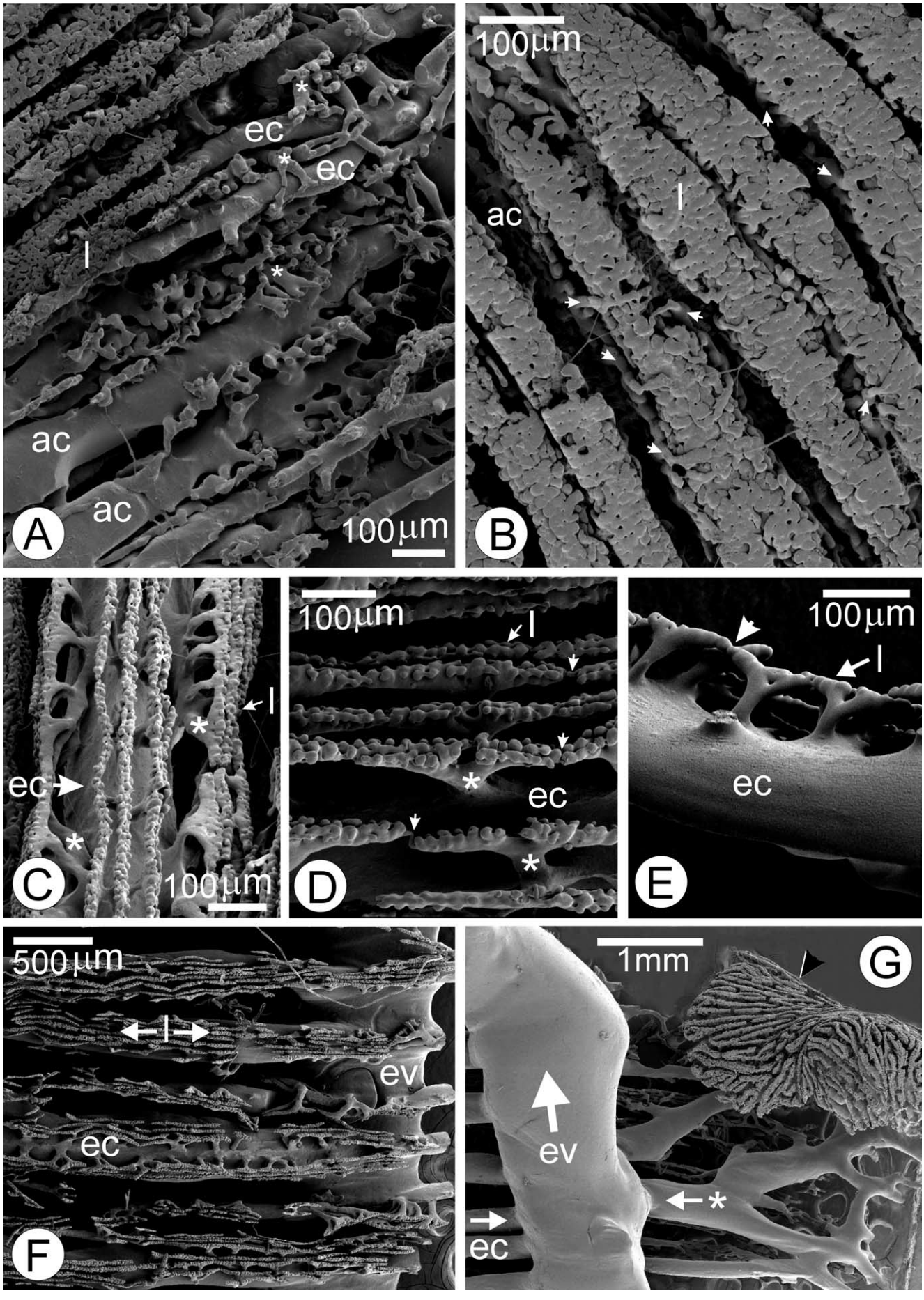
A
ec
ec
l
ac
ac
100μm
B
100μm
l
ac
C
ec
l
100μm
D
100μm
l
ec
E
100μm
l
ec
F
500μm
l
ev
ec
G
1mm
ev
ec

(prebranchial) blood. In two of these studies (Burggren and McMahon, 1981; Wheatly et al., 1986), venous samples were taken via the base of the chelae, i.e. from the anterior part of the infrabranchial sinus and should represent true venous blood as oxygenated abdominal blood does not reach the anterior infrabranchial sinuses. However, haemolymph samples taken from the posterior infrabranchial sinus would represent mixed blood with elevated oxygen. McMahon and Burggren (1979), took 'venous' samples directly from an unidentified abdominal sinus of *Coenobita clypeatus*. However, as they reported PvO_2 values very similar to those of Wheatly et al. (1986) (8.4 vs. 10 Torr, respectively), it is likely that their samples were drawn from a venous sinus in the abdomen. As the abdominal respiratory organ is non-functional in *B. latro* problems with mixed blood in the infrabranchial sinuses do not occur.

In an effort to demonstrate that the abdominal lungs were effective gas exchange organs, Borradaile (1903) and Harms (1932) removed the gills of *C. perlatus* and *C. rugosus*, respectively. The animals survived for several days and it was concluded that the abdominal respiration must be of considerable importance. Removal of the gills would obviously prevent the normal return of efferent blood from the abdomen to the pericardium (via the gills). As this route was closed, oxygenated haemolymph from the abdomen presumably flowed forwards into the anterior sinuses and then via the branchiostegal circulation to the heart. The vascular interconnections between the different respiratory organs in the terrestrial Anomura are obviously highly complex and detailed haemodynamic studies are needed in order to determine the relative contributions of each of the possible routes of venous return to normal circulation. The anatomical evidence, from corrosion casts, is certainly consistent with preferential return of haemolymph via the posterior gills. Studies are also needed in regard to the relative efficiencies of these different respiratory surfaces (branchiostegal lungs, gills and abdominal lung) and their contributions to gas exchange. The three gas exchange systems of *Coenobita* spp. appear to have a similar overall gas exchange capacity to that of *Birgus* and other land crabs as measured rates of oxygen consumption are of the same order (McMahon and Burggren, 1988).

The complex vascular network present in the dorsal abdomen of *Coenobita* is completely lacking in the aquatic hermit crabs. The dorsal abdominal integument of the aquatic *Paguristes oculatus* is covered by a relatively thick (although uncalcified) cuticle which is lined by a very well developed epidermis and musculature (Harms, 1932), similar to that found in the non-respiratory part of the dorsal integument of *C. perlatus* (Fig. 8(E)). Thus the abdominal lung present in the air-breathing *Coenobita* represents a novel adaptation for life on land.

In *Coenobita*, the air-channels in the respiratory patches are extremely closely spaced (300 cm^{-1}), thus dramatically increasing the surface area available for gas exchange. Indeed, the surface areas of the abdominal lungs of all three species are 4–7× those of their respective branchiostegites so that the total area of the gas exchange surfaces (abdominal and branchiostegal lungs plus gills) is likely to be of similar magnitude to those of the air-breathing brachyuran crabs (Greenaway, 1999). The walls of the respiratory grooves in *Coenobita* are covered by a thin cuticle and epithelium, lined by exchange lacunae. This arrangement is somewhat similar to that found in the lungs of the soldier crab, where exchange lacunae line the air-sacs (Farrelly and Greenaway, 1987). Interestingly, the blood/gas barrier across the respiratory grooves in the abdomen of *Coenobita* (200–350 nm) was significantly shorter (less than half) than that across their branchiostegites (700 nm) and may reflect the more complete adaptation of this organ for aerial gas exchange.

4.5. Evolution of respiratory systems in the coenobitidae

The family Coenobitidae contains only two genera, *Coenobita* (15 species) and *Birgus* (one species) and members of both are adapted for life on land (Little, 1983; Powers and Bliss, 1983; Hartnoll, 1988). The life histories of *Birgus* and *Coenobita* are very similar. In both, the glaucothoë larva returns to the shore already inhabiting a

Fig. 11. SEM of abdominal lung (A) *Coenobita rugosus*. High powered view of afferent cross-channels and exchange lacunae in abdominal lung. Note the flattened appearance of the afferent cross-channels (ac) with their distinctive marginal branches (*) that protrude up between the overlying efferent cross-channels (ec) and feed into the rows of lacunae (l) that lie just below the dorsal surface. (B) *Coenobita rugosus*. High powered view of exchange lacunae in abdominal lung. Note the small, finger-like afferent sinuses (arrows) that run up around the edges of the respiratory grooves and which feed into the dorsal lacunae (l), forming long lines of lacunae between the air-channels (dark spaces between rows of lacunae). The efferent cross-channels lie above the afferent cross-channels (ac) and are obscured by the overlying lacunae. (C) *Coenobita perlatus*. Dorsal view of an efferent cross-channel (ec). Multiple rows of collecting branches (*) drain the lacunae (l). (D) *Coenobita brevimanus*. High powered view of partially filled rows of lacunae (l) filled from the efferent side. Air-channels run in the spaces between the lines of lacunae. Rows of regularly spaced 'T-shaped' efferent collecting branches (*) joined end to end, drain the dorsal lacunae and then flow into the large efferent cross-channels (ec) below. Note that the connections between the ends of the 'Ts' appear quite constricted (arrows) and may help channel blood into the efferent cross-channels below. (E) *Coenobita brevimanus*. SEM of ventro-lateral view of an efferent cross-channel (ec), showing the smooth underside of the vessels and the 'T-shaped' collecting branches which drain haemolymph from the lines of dorsal lacunae (l). Note that the ends of the 'Ts' appear constricted (arrow head). (F) *Coenobita brevimanus*. SEM of vascular cast of abdominal lung. Dorsal view of efferent abdominal network, showing the multiple rows of lacunae (l) that drain into the efferent cross-channels (ec) and then into the large efferent veins (ev) on either side. (G) *Coenobita rugosus*, (efferent fill only). Ventral view of cast, showing the smooth underside of the efferent network. Here you can see the anterior portion of the left efferent vein (ev). Lateral branches (*) collect haemolymph from the sides of the abdominal lung, while the central cross-channels (ec) traverse the lung, linking the paired efferent veins either side. Arrows indicate direction of blood flow in efferent vessels. Note that the respiratory network also extends into the very elastic antero-lateral margin of the abdomen that seals against the shell (arrow head).

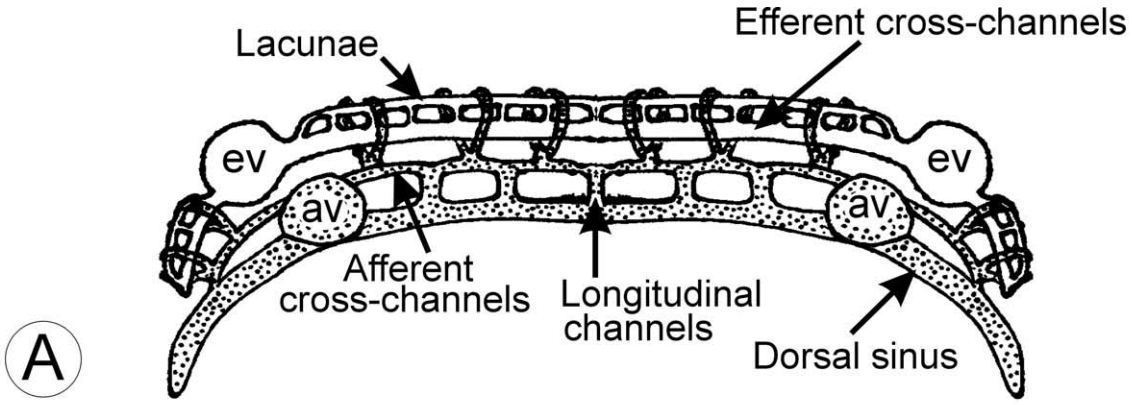
Lacunae
Efferent cross-channels
ev
ev
av
av
Afferent cross-channels
Longitudinal channels
Dorsal sinus
A

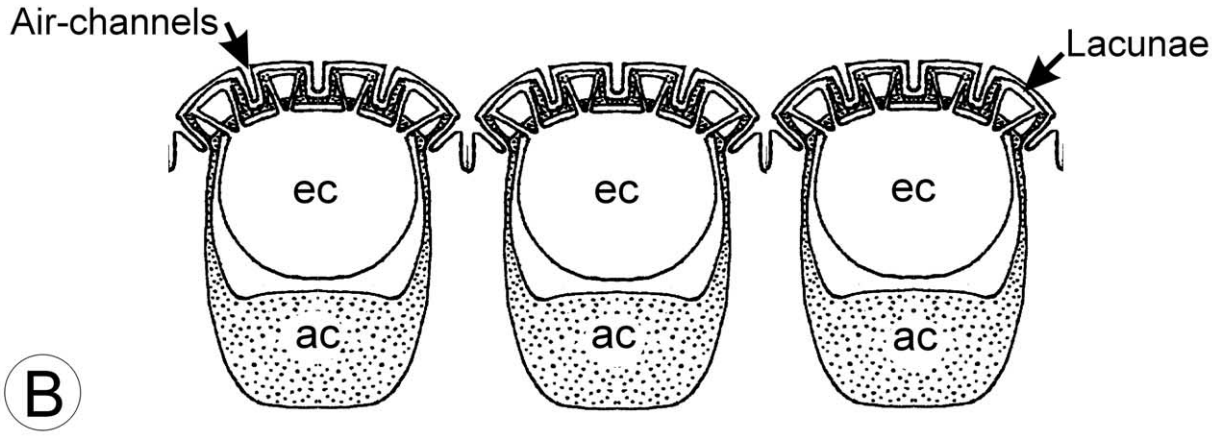
Air-channels
Lacunae
ec
ec
ec
ac
ac
ac
B

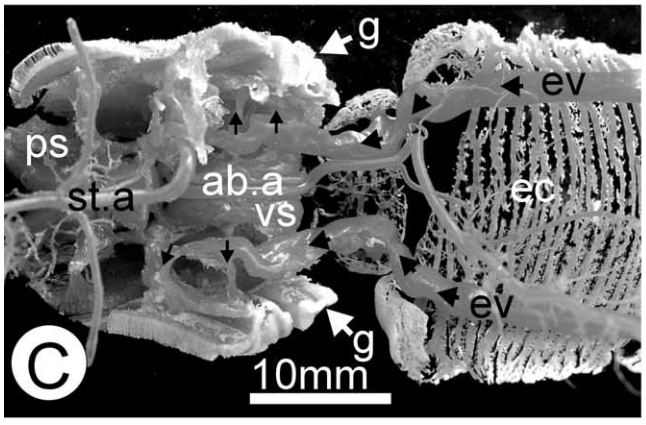
g
ev
ps
st.a
ab.a
vs
ec
ev
g
C
10mm

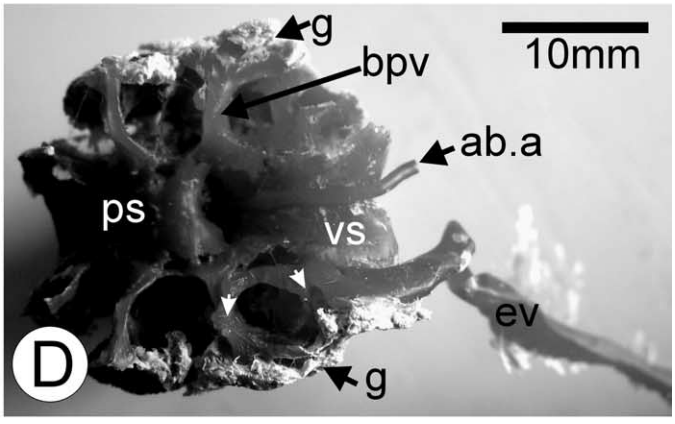
g
bpv
10mm
ab.a
ps
vs
ev
D
g

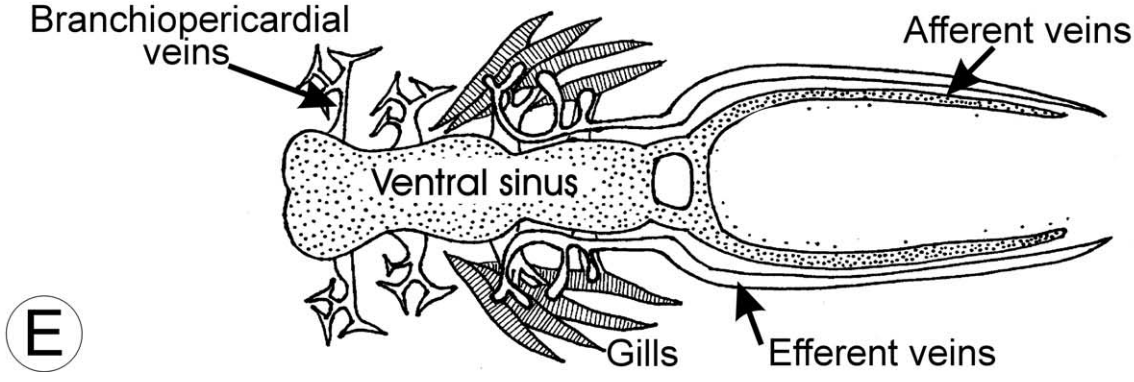
Branchiopericardial veins
Afferent veins
Ventral sinus
Gills
Efferent veins
E

tiny marine gastropod shell (Harms, 1938). *Birgus* soon abandons the mollusc shell and undergoes morphological changes to compensate for the loss of the shell but *Coenobita* spp. continue to utilise this form of protection throughout adult life. The transition of *Birgus* from the shell-inhabiting glaucothoë into the shell-less free-living form is described in detail by Harms (1932,1938) with the timing and length of these stages apparently dependent upon the availability of suitably sized shells. Thus *Birgus* may give up its protective marine shell almost as soon as it arrives on shore, or may transfer into larger land shells as it grows, (becoming more symmetrical with every moult) until it reaches a carapace length of 6–7 mm (2 years), after which they become free-living (Harms, 1938; Reese, 1968). Thus the final differentiation of *Birgus* is determined by the length of time spent in the shell, (where it remains *Coenobita*-like), only becoming fully differentiated and *Birgus*-like after adopting a free-living lifestyle. The main structural differences between adult *Coenobita* and *Birgus* that relate to respiratory changes include: the development and enlargement of the branchiostegal lung; the development of calcified plates on the abdomen; abdominal symmetry and thickening of abdominal integument (Harms, 1938; Hartnoll, 1988). The contractile lobes present on the antero-lateral edges of the abdomen in *Coenobita* are also present in young *Birgus* but are absent in adult *Birgus*. Prior to the assumption of a free-living lifestyle, *Birgus* and *Coenobita* are very difficult to distinguish morphologically (Harms, 1938).

The extreme plasticity of the adult morphology of *Birgus* was demonstrated by Harms (1938), who was able to extend the growth of captive animals in shells for up to 4 years (carapace length 21 mm) by providing increasingly larger shells. Likewise, if *C. clypeatus* is removed from its shell the morphology converges on that of *Birgus*. Thus the lungs are lengthened (although the lining remains smooth), the abdominal integument is thickened and the abdomen is held tucked under the body (Harms, 1932). Interestingly, Harms (1932) reported that in young *Birgus* that still live in a snail shell, the lung lining is smooth, but as the animal gets larger, it becomes increasingly evaginated, eventually forming branching lobes. Thus in its development, *Birgus* re-enacts the whole evolution of the lung from the simplest structure found in the coenobitids, up to the highly differentiated structures found in the adult. Indeed, if the outer surface of casts showing the major branchiostegal vasculature of *Coenobita* and *Birgus* are compared, it is clear that they share a similar basic morphology that consists of a series of interdigitating, branching vessels, joined by lacunae. It is only the morphology of the microvasculature that differs, which in *Birgus* has been greatly extended to supply the branching lobes of the lung, thereby significantly increasing the surface area available for gas exchange. So in *Birgus*, the lung circulation is much more highly developed, with both increased levels of branching and with many more exchange lacunae, resulting in a much more efficient lung.

The dorsal abdomen of *Birgus* retains the remnants of a respiratory vascular network, similar to that present in *Coenobita*, although clearly no longer functional in adult animals. However, such a system may be functional in young *Birgus*, before they discard their shells, thicken the abdominal integument and fully develop the branchiostegal lung (Harms, 1932). Further morphological and physiological studies on young *Birgus* during the transition from shell-carrying to free-living are needed to fully clarify the mechanisms driving this ontogenetic change. Thus abdominal breathing appears to have been developed before divergence of the coenobitid genera and the Coenobitidae share with the Paguroidea the pre-adaptation of a thin, uncalcified, abdominal integument, permitted by their shell carrying behaviour. Apart from the Coenobitidae, hermit crabs are not well adapted for terrestrial life although *Clibanarius* (Diogenidae) are active when exposed at low tide (Hartnoll, 1988; Little, 1983). It would be interesting to see if abdominal breathing has also developed to any extent in amphibious diogenids.

4.6. Conclusions

We conclude that the presence of a protective mollusc shell in the terrestrial hermit crabs has favoured the evolution of an abdominal lung whilst in its absence a branchiostegal lung has been developed. Thus *Coenobita*, which has retained a shell, has a very limited branchiostegal lung (growth restricted by shell) but has developed a complex abdominal lung. *Birgus*, which discards its shell

Fig. 12. (A) Schematic cross-section of the abdominal lung vasculature in the dorsal integument of *Coenobita*. Venous haemolymph is supplied to the lung from both the dorsal sinus (overlying hepatopancreas) and the afferent abdominal veins (av) to the afferent cross-vessels, which feed into lacunae lining the walls of the respiratory grooves. Oxygenated haemolymph is then collected by the efferent cross-channels, which flow either side into the large efferent abdominal veins (ev) and thence into the afferent branchial veins of the posterior gills. (B) Schematic longitudinal section through cross-vessels of the abdominal lung network. Venous haemolymph from the afferent cross-channels (ac) feeds around the overlying efferent cross-channels (ec) and into the lacunae lining the walls of the air-channels. Oxygenated haemolymph is then collected by the efferent cross-channels and flows into the efferent abdominal veins on either side. (C) *Coenobita brevimanus*. Ventral view of corrosion cast showing the efferent abdominal system. The paired abdominal veins (ev) flow directly into the thorax where they supply the last four gills (g) on either side. Note the smooth undersides of the efferent cross-channels (ec). Arrows indicate direction of blood flow in efferent veins. ab.a, abdominal artery, ps, pericardial sinus; st.a, sternal artery, vs. ventral sinus. (D) *Birgus latro*. Ventral view. This cast has been dissected to show the path of one efferent abdominal vein (ev) as it returns to the pericardial sinus (ps) via the posterior gills (g) and branchiopericardial veins (bpv). Small arrows indicate the junction of the efferent abdominal veins with the afferent branchial vessels of the posterior gills. ab.a, abdominal artery; vs, ventral sinus. (E) Schematic diagram showing the major distributing and collecting vessels in the abdominal lung of the terrestrial hermit crabs (ventral view). Note the direct return of the paired efferent abdominal veins to the afferent branchial vessels of the last four gills.

after its juvenile stages, has calcified and thickened its abdominal integument to give protection and reduce evaporative water loss, (thereby losing abdominal lung function), but has compensated by enlarging and developing its branchiostegal lungs. Both *Coenobita* and *Birgus* have extremely reduced gills. Increasing terrestrialisation in *Coenobita* is reflected by an increase in the number of segments involved with the abdominal lung, thus the more coastal species, *C. perlatus* and *C. rugosus* both utilize three segments, while in the more terrestrial *C. brevimanus* five abdominal segments have been incorporated, greatly increasing the surface area available for gas exchange. However, *Birgus* by giving up its protective shell has achieved even greater independence from the sea and must be regarded as having colonized land more successfully than *Coenobita*, in which mobility and growth are still restricted by a shell.

The elucidation of the abdominal lung will hopefully lay the groundwork for the re-examination of the respiratory physiology of the terrestrial hermit crabs, and so lead to a new appreciation and understanding of their adaptations to terrestrial life.

Acknowledgements

SEM of the corrosion casts was done in the Electron Microscopy Centre at La Trobe University, Vic. Aust., where we would like to gratefully thank Denise Fernando for all her assistance. Light Microscopy and TEM was done in the Microscopy Unit at the Peter MacCallum Cancer Institute, Vic. Aust., where we would like to thank Sarah Ellis and Manuela Palatsides for their support. SEM of gills was done at the Electron Microscopy Unit at the University of New South Wales.

References

Borradaile, L.A., 1903. Land crustaceans, in: Gardiner, J.S. (Ed.), The Fauna and Geography of the Maldive and Laccadive Archipelagoes, vol. 5. Cambridge University Press, Cambridge, pp. 64–100.

Bouvier, E.L., 1890a. Sur la respiration et quelques dispositions organiques des paguriens terrestres du genre Cénobite. Bulletin de la Société de Philomatique de Paris 8, 194–197.

Bouvier, E.L., 1890b. Sur le cercle circulatoire de la carapace chez les Crustacés Décapodes. Comptes rendus hebdomaires de séances de l'Academie des sciences, Paris 110, 1211–1213.

Burggren, W.W., McMahon, B.R., 1981. Hemolymph oxygen transport, acid-base status, and hydromineral regulation during dehydration in three terrestrial crabs, *Cardisoma*, *Birgus*, and *Coenobita*. Journal of Experimental Zoology 218, 53–64.

Davie, P.J.F., 2002. Crustacea: Malacostraca Eucarida (Part 2) Decapoda—Anomura, Brachyura, Zoological Catalogue of Australia 19.3B. CSIRO Publishing, Collingwood, Australia.

Drach, P., 1930. Étude sur le système branchiale des crustacés Décapodes. Archives d' anatomie microscopique et de morphologie experimentale 26, 83–133.

Farrelly, C., Greenaway, P., 1987. The morphology and vasculature of the lungs and gills of the soldier crab, *Mictyris longicarpus*. Journal of Morphology 193, 285–304.

Farrelly, C.A., Greenaway, P., 1992. Morphology and ultrastructure of the gills of terrestrial crabs (Crustacea, Gecarcinidae and Grapsidae): adaptations for air-breathing. Zoomorphology 112, 39–49.

Farrelly, C.A., Greenaway, P., 1993. Land crabs with smooth lungs: Grapsidae, Gecarcinidae, and Sundathelphusidae: ultrastructure and vasculature. Journal of Morphology 215, 245–260.

Greenaway, P., 1984. The relative importance of the lungs and gills in gas exchange of amphibious crabs of the genus *Holthuisana*. Australian Journal of Zoology 32, 1–6.

Greenaway, P., 1998. Physiological diversity and the colonization of land, in: Schram, F.R., von Vaupel Klein, J.C. (Eds.), Proceedings of the Fourth International Crustacean Congress, Amsterdam, The Netherlands, July 20–24, 1998, vol. 1. Brill Academic Publishers, Leiden, pp. 823–842.

Greenaway, P., 2003. Terrestrial adaptations in the Anomura (Crustacea: Decapoda). Memoirs of Museum Victoria 60, 13–26.

Greenaway, P., Farrelly, C.A., 1984. The venous system of the terrestrial crab *Ocypode cordimanus* (Desmarest 1825) with particular reference to the vasculature of the lungs. Journal of Morphology 181, 133–142.

Greenaway, P., Morris, S., McMahon, B.R., 1988. Adaptations to a terrestrial existence by the robber crab, *Birgus latro*: II. In vivo respiratory gas exchange and transport. Journal of Experimental Biology 140, 493–509.

Harms, J.W., 1929. Die Realisation von Genen und die consecutive Adaption. I. Phasen in der Differenzierung der Anlagenkomplexe und die Frage der Landtierwerdung. Zeitschrift für wissenschaftliche Zoologie 133, 211–397.

Harms, J.W., 1932. Die Realisation von Genen und die consecutive Adaption. II *Birgus latro* L. als Landkrebs und seine Beziehungen zu den Coenobiten. Zeitschrift für wissenschaftliche Zoologie 140, 167–290.

Harms, J.W., 1938. Lebensablauf und Stammesgeschichte des *Birgus latro* L. von der Weihnachtsinsel. Jenaische Zeitschrift für Naturwissenschaft 71, 1–34.

Hartnoll, R.G., 1988. Evolution, systematics, and geographic distribution, in: Burggren, W.W., McMahon, B.R. (Eds.), Biology of the Land Crabs. Cambridge University Press, Cambridge, pp. 6–53.

Jackson, H.G., 1913. *Eupagurus*, in: Herdman, W.A. (Ed.), Liverpool Marine Biology Committee Memoirs on Typical British Marine Plants and Animals, vol. XXI. Williams and Nordgate, London, pp. 1–79.

Little, C., 1983. The Colonisation of Land, Origins and Adaptations of Terrestrial Animals. Cambridge University Press, Cambridge pp. 84–87.

Maitland, D.P., 1986. Crabs that breathe air with their legs—*Scopimera* and *Dotilla*. Nature 319, 493–495.

McLaughlin, P.A., 1980. Comparative Morphology of Recent Crustacea. Freeman, San Francisco.

McMahon, B.R., Burggren, W.W., 1979. Respiration and adaptation to the terrestrial habitat in the land hermit crab *Coenobita clypeatus*. Journal of Experimental Biology 79, 281–285.

McMahon, B.R., Burggren, W.W., 1988. Respiration, in: Burggren, W.W., McMahon, B.R. (Eds.), Biology of the Land Crabs. Cambridge University Press, New York, pp. 249–297.

Morris, S., Greenaway, P., 1990. Adaptations to a terrestrial existence by the robber crab, *Birgus latro* L.V. The activity of carbonic anhydrase in gills and lungs. Journal of Comparative Physiology B 160, 217–221.

Pearson, J., 1908. Cancer, Liverpool Marine Biology Committee Memoirs on Typical British Marine Plants and Animals, vol. XVI. Williams and Nordgate, London.

Pike, R.B., 1947. *Galathea*, in: Daniels, R.J. (Ed.), Liverpool Marine Biology Committee Memoirs on Typical British Marine Plants and Animals, vol. XXXIV. The University Press of Liverpool, pp. 1–179.

Powers, L.W., Bliss, D.E., 1983. Terrestrial adaptations, in: Vernberg, J., Vernberg, W.B. (Eds.), The Biology of Crustacea, vol. 8. Academic Press, New York, pp. 271–333.

Reese, E.S., 1968. Shell use: an adaptation for emigration from the sea by the coconut crab. Science 161, 385–386.

Storch, V., Welsch, U., 1975. Über Bau and Funktion der Kiemen und Lungen von *Ocypode ceratophthalma* (Decapoda: Crustacea). Marine Biology 29, 363–371.

Storch, V., Welsch, U., 1984. Electron microscopic observations on the lungs of the coconut crab, *Birgus latro* (L.) (Crustacea, Decapoda). Zoologischer Anzeiger 212, 73–84.

Taylor, H.H., Greenaway, P., 1979. The structure of the gills and lungs of the arid-zone crab, *Holthuisana* (*Austrothelphusa*) *transversa* (Brachyura: Sundathelphusidae) including observations on arterial vessels within the gills. Journal of Zoology, London 189, 359–384.

Taylor, H.H., Taylor, E.W., 1992. Gills and lungs: the exchange of gases and ions, in: Harrison, F.W., Humes, A.G. (Eds.), Microscopic Anatomy of Invertebrates, Decapod Crustacea, vol. 10. Wiley-Liss, New York, pp. 203–293.

von Raben, K., 1934. Veränderungen in Kiemendeckel und in den Kiemen einiger Brachyuren (Decapoden) im Verlauf der Anpassung an die Feuchtluftatmung. Zeitschrift für wissenschaftliche Zoologie 145, 425–461.

Wheatly, M.G., McMahon, B.R., Burggren, W.W., Pinder, A.W., 1986. Haemolymph acid-base, electrolyte and gas status during sustained voluntary activity in the land hermit crab (*Coenobita compressus*). Journal of Experimental Biology 125, 225–243.